This is to certify that the

thesis entitled

SYNTHESIS AND CHARACTERIZATION OF
INCLUSION COMPLEXES OF α-CYCLODEXTRIN
AND $(AB)_n$ BLOCK COPOLYMERS

presented by

Kirk L. Olson

has been accepted towards fulfillment
of the requirements for

M.S. degree in CHEMISTRY

Major professor

Date 21 August 2001

SYNTHESIS AND CHARACTERIZATION OF INCLUSION COMPLEXES OF α-CYCLODEXTRIN AND $(AB)_n$ BLOCK COPOLYMERS

By

Kirk L. Olson

A THESIS

Submitted to
Michigan State University
in partial fulfillment of the requirements
for the degree of

MASTER OF SCIENCE

Department of Chemistry

2001

ABSTRACT

SYNTHESIS AND CHARACTERIZATION OF INCLUSION COMPLEXES OF α-CYCLODEXTRIN AND $(AB)_n$ BLOCK COPOLYMERS

By

Kirk L. Olson

Cyclodextrins thread onto polymer chains to form inclusion complexes, especially when the polymer is hydrophobic relative to the solvent. Selective threading might occur when the polymer architecture contains both hydrophobic and hydrophilic segments. α-Cyclodextrin formed crystalline inclusion complexes with $(AB)_n$ microblock copolymers, where the A block is a linear alkyl segment containing a single double bond and the B block is an exact length segment of polyethylene oxide. The complexes were isolated and characterized by solution and solid state NMR, XRD, DSC, and TGA. Each method confirmed complex formation and showed that the physical properties of the complexes are distinct from its individual components. The X-ray data are consistent with known inclusion complexes that have a channel or column crystal structure. The stoichiometry of complex formation, 2.3 α-cyclodextrin rings per polymer repeat unit, was determined by NMR analysis of the complexes, and from an analysis of the yields of inclusion complexes. The data suggest that the inclusion complex stoichiometry is defined by the increasing insolubility of the polymer-cyclodextrin complex. Solid state NMR suggests that there is a slight preference for threading onto hydrophobic segments of the $(AB)_n$ polymer.

To my family

ACKNOWLEDGEMENTS

First and foremost I would like to express my thanks and gratitude to my parents and my sister for their undeniable love and support for me throughout my graduate school experience. I write and dedicate this thesis for you.

I would also like to thank my advisor, boss, and friend, Gregory L. Baker, for his knowledge, support, and guidance throughout the course of this research. Baker group members have made this an enjoyable experience and I hope to stay in touch with all. Gao (woo?) thanks for mentoring me and being a true friend. Micah, Chun, JB, and Tianqi you have been wonderful sources of knowledge and fun. Erin thanks for being a lunch mate and a friend going through the same experiences. Fadi.... thanks for some good laughs and a source of bad coffee!

Finally I would like to thank all my friends and family for their support! It has been a fun ride! I have really enjoyed my graduate school experience and met some true friends. Thanks, and God bless all.

TABLE OF CONTENTS

LIST OF ABBREVIATIONS

ADMET	Acyclic diene metathesis
BA	Polybutyl acrylate
CD	Cyclodextrin
$C_xEO_yC_x$	See page 11
$[C_x\pi C_xEO_y]_n$	See page 11
CP	Cross polarization
DSC	Differential scanning calorimetry
DD	Dipolar decoupling
G	Guest molecule
GPC	Gel permeation chromatography
H/G	Host-guest complex
H	Host molecule
IC	Inclusion complex
MAS	Magic angle spinning
M_n	Number average molecular weight
M_w	Weight average molecular weight
NMR	Nuclear magnetic resonance
PCL	Poly (ε-caprolactone)
PDXL	Poly (1,3-dioxolane)
PE	Polyethylene
PEG	Polyethylene oxide
PIB	Polyisobutylene
PPO	Polypropylene oxide
PS	Polystyrene
ROMP	Ring opening metathesis polymerization
TGA	Thermogravimetric analysis
T_c	Crystallization temperature
T_g	Glass-transition temperature
T_m	Melting point
XRD	X-ray diffraction
α-CD	Six glucose repeat units in CD
β-CD	Seven glucose repeat units in CD
γ-CD	Eight glucose repeat units in CD
δ	Chemical shift
λ	Wavelength
θ	Diffraction angle

LIST OF FIGURES

LIST OF SCHEMES

LIST OF TABLES

CHAPTER 1

Introduction

1.1 Cyclodextrins

Cyclodextrins (CDs) are a series of cyclic oligosaccharides consisting of 6, 7, 8, or larger (10, 14, or 26) glucose units joined by α-1,4-glycosidic linkages. Cyclodextrins are designated by the use of Greek letters (α, β, γ…), which correspond to the number of glucose units in the CD ring. The smallest cyclodextrin contains six (α) glucose units. Cyclodextrins **(Figure 1.1)** resemble a hollow truncated cone with primary hydroxyl groups located on the narrow side of the cone, and secondary hydroxyl groups on the wide rim of the cone. The hydroxyl groups located on the exterior of the cone make CDs hydrophilic and soluble in aqueous solutions, but the interior cavities of CDs are hydrophobic allowing CDs to incorporate small molecules or guests to form host-guest inclusion complexes (ICs).[1]

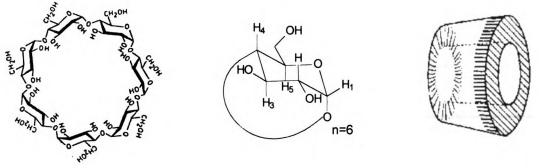

Figure 1.1. Representative structures of cyclodextrin as illustrated by Szejtli.[2]

Villiers discovered cyclodextrin in 1891 while he was digesting starch with a microorganism, *Bacillus amylobacter*.[1] He collected two distinct crystalline products (α and β-CD) that he called cellulosines. In 1904, Schardinger, the first person to actually characterize the crystalline extracts produced from starch, determined that the

cellulosines were actually cyclic oligosaccharides. Because of his discovery, CDs are sometimes referred to as Schardinger dextrins.[1] The procedure used for the synthesis of CDs today is very similar to that by Villiers, but involves the use of a different microorganism, *Bacillus macerans*, which produces the cyclodextrin glucosyl transferase enzyme (CGT-ase).[2] α, β, and γ-CDs are formed upon the addition of CGT-ase to a prehydrolyzed starch solution. The glycosyl transferase enzyme acts by fragmenting the starch helix and then linking the ends of the fragment to form cyclic oligosaccharides. From the starch digests, the components of the complicated mixture of CDs can be separated by the use of selective complex forming agents.[2] Toluene is used to complex with β-CD, 1-decanol with α-CD, and cyclohexadecenol for the larger γ-CD. After complexation with these agents, the insoluble complexes are separated from the mixture by filtration, washed and then the complex agent is extracted from the CD to give the pure product. Today CDs are produced in quantities of greater than 1000 tons per year, and in greater than 99% purity.[2] Some of the characteristics and physical properties of commercially available CDs are listed in **Table 1.1.**

Table 1.1. Characteristics of α, β, and γ-cyclodextrins.[2]

	α	β	γ
Number of glucose units	6	7	8
Molecular weight	972	1135	1297
Solubility in water, g 100 mL^{-1} at room temp	14.5	1.85	23.2
$[\alpha]_D$ 25°C	150 ± 0.5	162.5 ± 0.5	177.4 ± .5
Cavity diameter, Å	4.7-5.3	6.0-6.5	7.5-8.3
Height of torus, Å	7.9 ± 0.1	7.9 ± 0.1	7.9 ± 0.1
Diameter of outer periphery, Å	14.6 ± 0.4	15.4 ± 0.4	17.5 ± 0.4
Approx. volume of cavity, $Å^3$	174	262	427
Crystal water, wt %	10.2	13.2-14.5	8.13-17.7

The structure of CDs (**Figure 1.1**) and the cavity diameters listed in **Table 1.1** suggests the possibility that CD molecules could form a complex (two or molecules held together in a definable structural relationship) with other molecules in the interior cavity of cyclodextrin. In the early 1950's, Cramer discovered that CD and small organic molecules could form complexes, and upon complexation with CD, the guest molecule obtained certain benefits such as alteration of the solubility of the guest compound, stabilization against the effects of heat, light, and oxidation, and also a reduction of volatility.[3] Because of these benefits, CDs are now employed in numerous industrial applications including the pharmaceutical, food and cosmetic industries.[4] **Figure 1.2** describes the breakdown of CD-related papers in terms of their relevance to industrial applications for the year 1996.[2] The most common application of cyclodextrins is in the pharmaceutical industry where drugs complexed with CD are found to have enhanced solubility, stability, and bioavailability of the drug molecules. **Table 1.2** summarizes some of the uses of CD found in the pharmaceutical, food, and cosmetic industries.

Cyclodextrin is not only important because of its numerous applications found in industry, but also because CD complexes have become model systems for studying the non-covalent attractive forces that are found in complex biological systems, such as enzymes, proteins, and DNA. Supramolecular structures, catenanes and rotaxanes, can be made that mimic similar types of structures that are found in nature. Using the complexing ability of CDs, one can easily synthesize these supramolecular structures, which are not readily prepared by other methods. Recently, CD has been used as types of ligands or sites for molecular recognition of various chemical compounds, which has given renewed interest in the possible uses of cyclodextrin. In the work described in this

thesis, CD has been employed to study the properties of polymer inclusion complex formation with an amphiphilic multiblock copolymer.

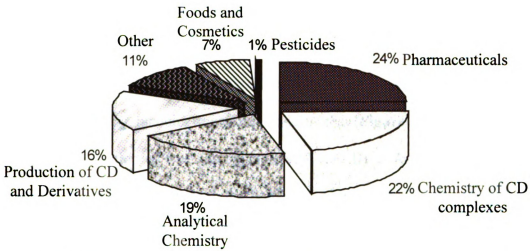

Figure 1.2. Distribution of CD relevant papers published in 1996 by *Cyclodextrin News*.[2]

Table 1.2. Selected applications of cyclodextrins in industry.[2,4]

Food	
Application	**Use of CD**
Cinnamon-flavored apples	Stabilize flavor
Flavored tea	Stabilize flavor
Peppermint-flavored chewing gum	Flavor delivery
Mustard oil steak sauce	Improve solubility
Acetic acid	Convert to a powder
Cinnamon-flavored chewing gum	Flavor delivery
Aloe-containing beverage	Mask bitterness
Vitamin B fruit juice beverage	Mask vitamin odor
Processed cheese	Cholesterol removal
Pharmaceutical	
Itraconazole	Increased solubility
Piroxicam	Reduce irritation
PGE1	Increased stability
PGE2	Solubility, stability
Hydrocortisone	Increased solubility
Cosmetics and Personal Care Items	
Artificial tanning lotion	Stability, mask odor
Powdered hair bleach	Stability
Perfume	Prolonged release
Skin cleanser	Tocopherol carrier

1.2 Block copolymer properties in general

Block copolymers are macromolecules comprised of two dissimilar repeat units (A and B) that are connected (chemically bonded) to one another. Copolymers can be synthesized in a variety of patterns that are distinguished by the number of blocks per molecule (**Figure 1.3**). The blocks in these copolymers can be arranged so that repeating units can be alternating, random, or grafted to one another (**Figure 1.4**).[5]

The combination of two homopolymers (A and B) to form a block copolymer allows the polymer to not only have the properties of the individual segments, but also give rise to new properties not found in a simple blend of polymers A and B. In a blend, polymers A and B phase separate at the macroscopic level as a consequence of the positive free energy change for mixing (ΔG_{mix}).

$$\Delta G_{mix} = \Delta H_{mix} - T\Delta S_{mix} \qquad \textbf{Equation 1.1}$$

When two polymers are mixed together, the entropy of mixing (ΔS_{mix}) is very small due to the high molecular weight of the polymers. In most cases, the enthalpy of mixing (ΔH_{mix}) is slightly positive, which leads to an overall slightly positive free energy change (ΔG_{mix}) that results in incompatibility or phase separation. In block copolymers, aggregation of individual polymer blocks with one another leads to phase separation, but because the blocks are chemically linked to one another, macroscopic phase separation is inhibited. The Flory-Huggins parameter (χ) is defined as,

$$\chi = \Delta H_{mix}/kTN_A v_B \qquad \textbf{Equation 1.2}$$

where N_A is the number of repeat units in block A, and v_B is the volume fraction of block B. χ is a dimensionless parameter that describes the interactions or compatibility

between blocks A and B. If χ is negative, polymers are miscible with one another (homogenous), but if χ is positive the copolymers will phase separate.

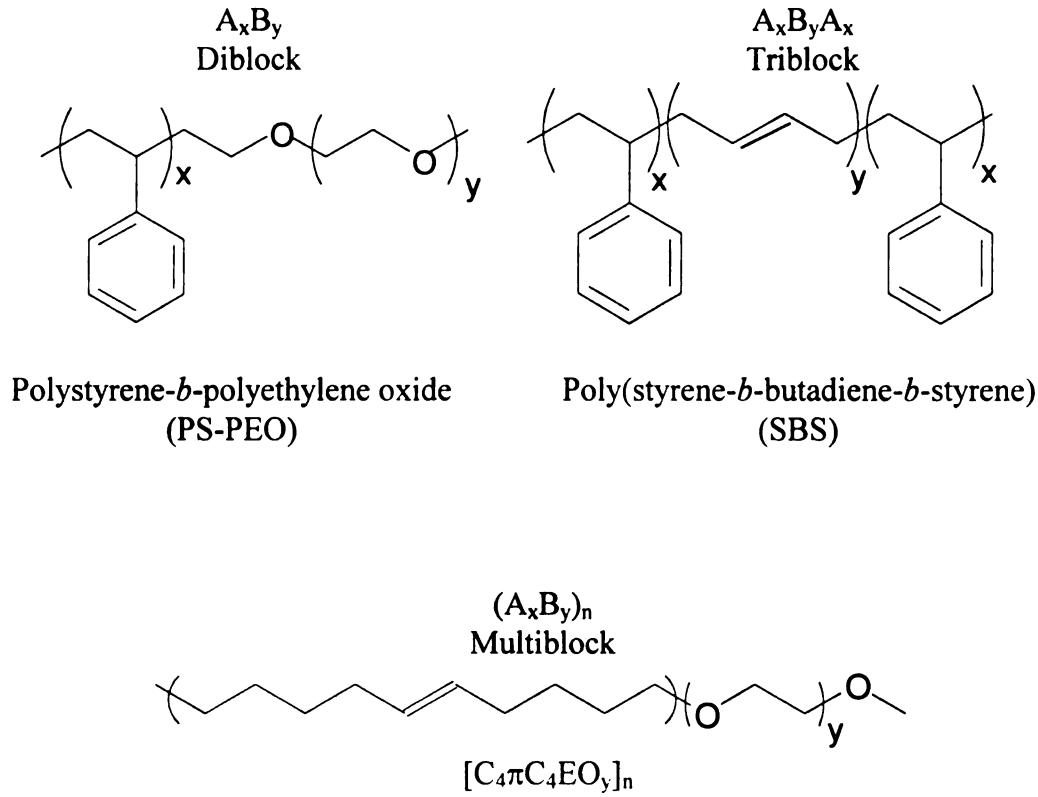

Figure 1.3. Types and examples of block copolymers.

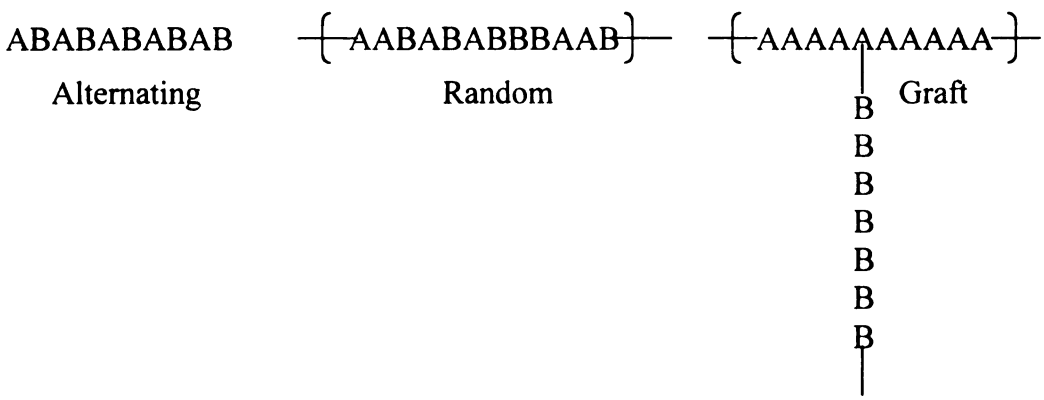

Figure 1.4. Alternating, random, and grafted block copolymers.

Incompatibility of blocks leads to the formation of new polymer structures (morphologies) that depend on the composition of the blocks in the copolymer (**Figure 1.5**). If the volume fractions, *v*, of the blocks are nearly equal, layered lattices or lamellae (**Figure 1.5**, C) form, but if the volume fraction of one of the blocks is larger than the other, then spheres (A), cylinders (B), or bicontinuous structures can be formed. Phase diagrams can be made that describe the change in the micro-domain structure of the polymer as a function of the volume fraction of the blocks.

Figure 1.5. Morphologies of AB block copolymers. White portions represent block A, while dark portions represent block B of the AB polymer.[6]

Block copolymers are synthesized to alter the properties of a homopolymer to achieve desired properties such as decreased crystallinity or improvements in the impact resistance. The most common application of block copolymers is as thermoplastic elastomers. Thermoplastic elastomers are polymers that possess thermally reversible chemical or physical cross-links. An example of a thermoplastic elastomer is the ABA triblock copolymer poly(styrene-*b*-butadiene-*b*-styrene) (SBS, **Figure 1.3**).[5,7] Styrene and butadiene are incompatible with each another so they form separate phases joined at the junctures where the various blocks are connected. This results in an elastomeric material with soft (polybutadiene) and hard (polystyrene) segments. The glassy polystyrene phases act as physical cross-links that are lost when the copolymer is heated

above 109 °C, the glass transition of polystyrene. Thermoplastic elastomers are used in automobile tires, footwear, and various automobile parts. Another example of a thermoplastic elastomer is *Spandex* or *Lycra*, which consists of a urea (hard block) and diamine (soft block).[5]

1.2.1 Amphiphilic materials

A similar combination of incompatible blocks is found in amphiphilic block copolymers. The term amphiphilic describes molecules that love both aqueous and non-aqueous (oil) phases. The water-loving phase of an amphiphilic material is hydrophilic, while the non-aqueous (water-hating or oil-loving) phase is hydrophobic.[8] Amphiphilic materials have the unique ability to form self-assembled aggregates (micelles) when dissolved in aqueous solutions (**Figure 1.6**). The driving force for the formation of micelles is the minimization of contact of the hydrophobic segments with the aqueous phase. As the concentration of the amphiphilic molecules increases, the hydrophobic portions of the molecules aggregate to form solutions that contain both non-aggregated species as well as clusters of various sized aggregates. At high concentrations, networks composed of interpenetrating clusters are formed. The reverse process can happen when the amphiphile is exposed to an oil or lipophilic solvent. The hydrophilic blocks associate to form micelles with the outer-shell of the micelle composed of the hydrophobic block. The ability of amphiphilic block copolymers to form micelles has led to the use of these materials for the transportation of dyes in printing technology as well as drug carrier systems.[8]

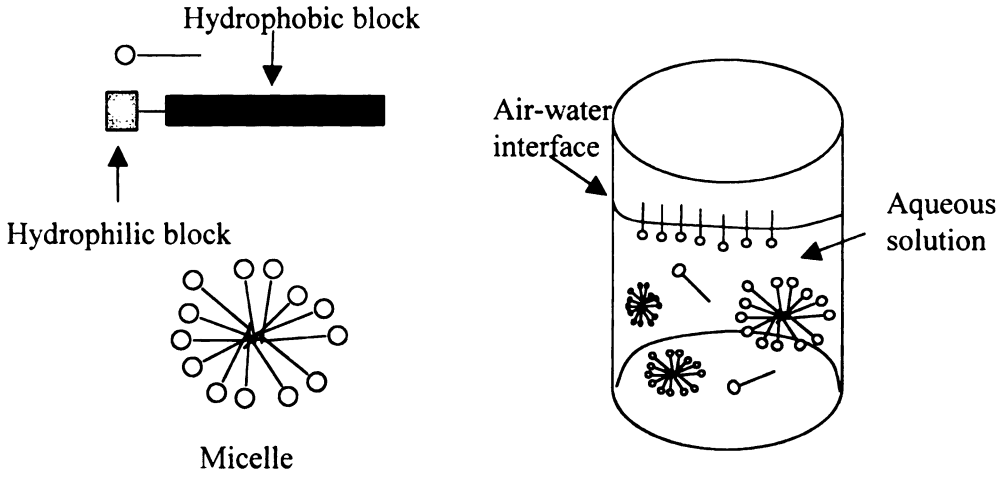

Figure 1.6. Structure of amphiphilic block copolymers and the formation of micelles in aqueous solutions.

Amphiphilic block copolymers can act as surfactants (a compound that reduces the interfacial tension between two liquids or a liquid and a solid) and therefore have applications as detergents, emulsifiers, and dispersants. There are three major classes of surfactants (**Figure 1.7**), which are named according to the type of hydrophilic group they contain: ionic (both cationic and anionic), zwitterionic, and nonionic. Ionic surfactants have charged hydrophilic groups such as carboxylate ions (example: soaps) or protonated amines. Zwitterionic surfactants contain both positive and negatively charged hydrophilic groups, while the hydrophilic groups in nonionic surfactants contain no charges but consist mainly of hydroxyl groups or ethers. The ABA triblock copolymers made from hydrophilic poly(ethylene oxide) (PEO) and hydrophobic poly(propylene oxide) (PPO) (**Figure 1.7**) are common examples of amphiphilic block copolymers that are used as nonionic surfactants. These surfactants are commercially available, and are known as Pluronics, Polaxamers, or Synperonics. Numerous researchers have studied

these amphiphilic polymers to determine their phase behavior in selective solvents (both "water" and "oil") for one of the blocks.[9,10]

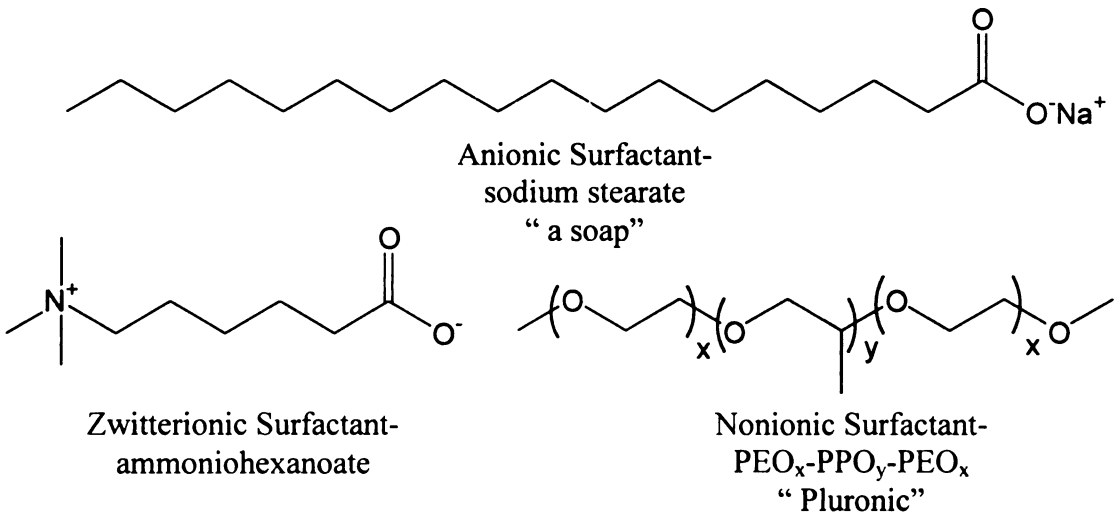

Figure 1.7. Types and examples of surfactants.

1.2.2 Synthesis and properties of $(AB)_n$ copolymers and ABA triblock oligomers

The structures of the $(AB)_n$ block copolymers and ABA triblock oligomers used in this research are shown in **Scheme 1.1**. The $(AB)_n$ block copolymers are abbreviated as $[C_x\pi C_xEO_y]_n$, where C_x corresponds to x methylene units, π represents the two carbon atoms of the double bond, and EO_y refers to y ethylene oxide repeat units. The ABA triblock oligomers have a similar shorthand notation and are abbreviated as $C_xEO_yC_x$. As seen in **Scheme 1.1**, the A block represents a linear alkyl segment, or a linear alkyl segment containing a single double bond and the B block corresponds to an oligomeric segment of ethylene oxide. These polymers have been previously synthesized and have been found to have very interesting properties.[11,12] The polymers are amphiphilic in character with the ethylene oxide segment (B block) being hydrophilic, and the alkyl segment (A block) being hydrophobic. The dual nature of these polymers allows for the

practical application of these polymers as nonionic surfactants. Additionally because the polymers contain PEO blocks, these polymers can be used as solid polymer electrolytes when doped with various Li^+ salts.[13]

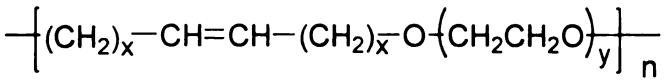

$[C_x\pi C_xEO_y]_n$

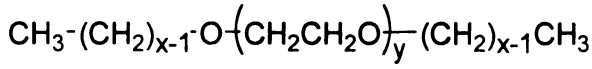

$C_xEO_yC_x$

Scheme 1.1. Generic structure of $(AB)_n$ polymer and ABA model compounds used in this research

The polymers were synthesized by Acyclic Diene Metathesis (ADMET) polymerization **(Scheme 1.2)** of oligoethylene oxide α,ω-dialkenyl ethers using Schrock's molybdenum alkylidene catalyst. ADMET polymerization is a step growth polymerization of dienes. The polymerization cycle involves the formation of metallocyclobutane intermediates that lead to dimer, trimer, and eventually high molecular weight polymer formation.[14] Ethylene is a volatile by-product of the reaction and is easily removed under vacuum to drive the equilibrium of the reaction to favor the condensation process. The most widely used catalysts for ring opening metathesis (ROMP) and ADMET polymerizations are those developed by Grubbs[15] and Schrock[16] (**Figure 1.8**). Grubb's ruthenium catalysts and the molybdenum and tungsten catalysts of Schrock have been widely used for the synthesis of unsaturated polyethers, esters, carbonates, and other $(AB)_n$ polymer structures.

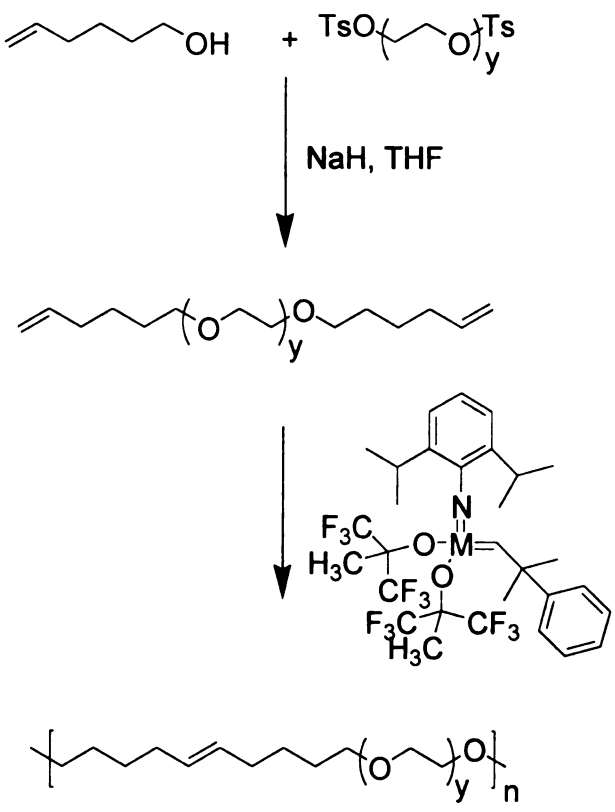

Scheme 1.2. Synthesis of $(AB)_n$ multiblock copolymers.

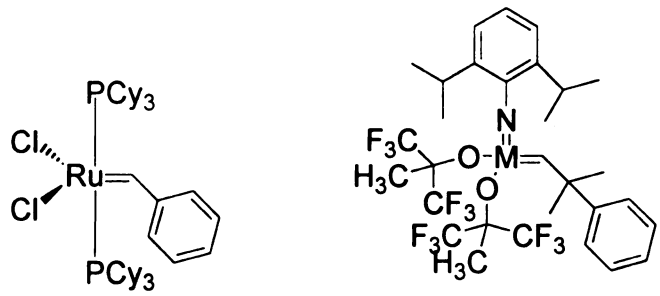

Figure 1.8. Grubbs and Schrock's metal alkylidene metathesis catalysts.

A series of exact length triblock ABA oligomers **(Scheme 1.3)** with the generic structure $H(CH_2)_x(OCH_2CH_2)_y(CH_2)_xH$, were used to help understand the crystallization and solubility behavior of the $(AB)_n$ multiblock copolymers. The ABA triblock oligomers were synthesized **(Scheme 1.3)** by treating an appropriate exact length oligoethylene glycol with sodium hydride, followed by addition of two equivalents of the desired alkyl bromide. Depending on the chain lengths of x and y, the products of the reaction ranged from viscous oils to crystalline solids.[17,18]

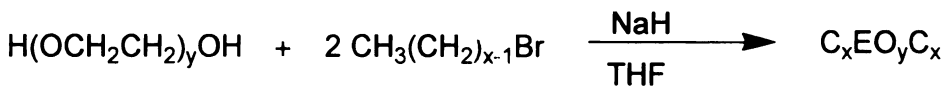

Scheme 1.3. Synthesis of ABA triblock oligomers.

Exact length oligoethylene glycols were used in the synthesis of both the $(AB)_n$ block copolymers and the ABA triblock oligomers to help increase the regularity and crystallinity of the B block. If ethylene oxide chain lengths with an average value (random distribution) were used, the packing of the chains would be irregular, causing a decrease in the crystallinity of the block copolymer and triblock oligomers. In addition, exact length ethylene oxide chains enables systematic studies of the evolution of the physical properties of polymers and oligomer (ex: solubility) with changes in the length of the ethylene oxide segment. Oligoethylene glycols are commercially available up to six repeat units but longer exact length EO_y chains need to be synthesized. A modified version of the approach of Keegstra[19] was used to prepare glycols where **y** is 6-10 and 14. The route to these exact length oligoethylene glycols is outlined in **Scheme 1.4.**

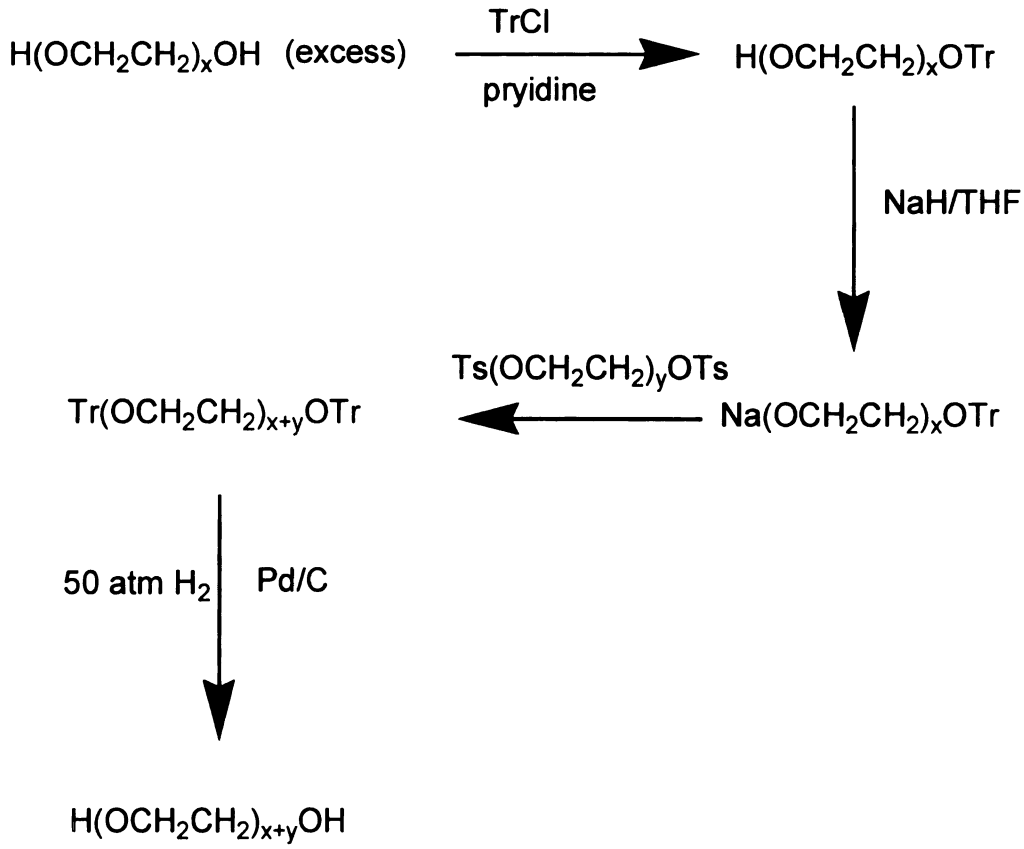

Scheme 1.4. Synthesis of exact length oligoethylene glycols.

The polymers and triblock oligomers were used in this research to study the effect that inclusion complex formation with cyclodextrin has on their physical properties. CD is known to thread on various hydrophilic and hydrophobic polymers, so the amphiphilic nature of the $(AB)_n$ block copolymers and ABA oligomers could lead to interesting structures when cyclodextrin preferentially threads onto one of the blocks.

1.3 Host-Guest chemistry

The terms "host" and "guest" are used to name complexing partners in synthetic organic chemistry.[20] A host is defined as an organic molecule or ion whose binding sites converge in the complex, while a guest is a molecule whose binding sites diverge in the complex.[20] Complexing partners are not unique or original to organic chemistry. Metal ions (H) and ligands (G) are complexing partners found in inorganic chemistry, while enzymes (H) and substrates (G) are complexing partners found in biochemistry. Host-Guest (H-G) complex chemistry is based on the ideals of the organizational ability found between membranes and enzymes. In 1894 Emil Fischer proposed the Lock and Key model (**Figure 1.9**) to describe the interactions between the active site of an enzyme and a site-specific substrate.[21] The shape of the reacting substrates and the enzyme's active site fit together like a key that opens a lock.

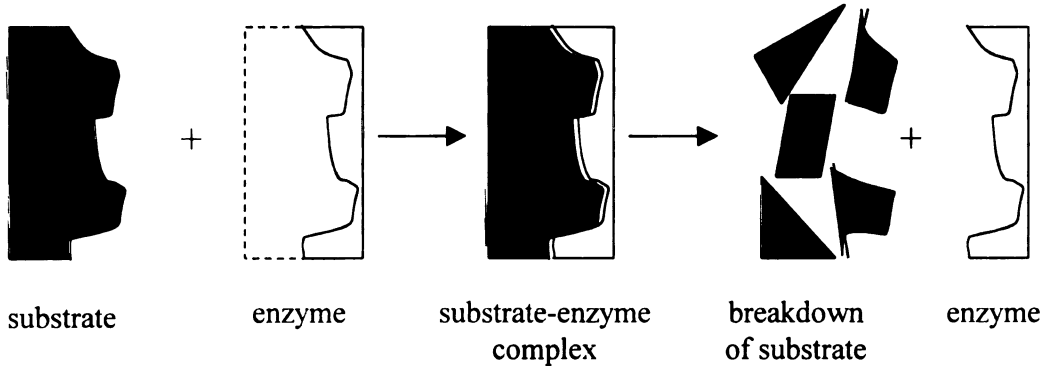

Figure 1.9. Emil Fischer's Lock and Key Model for enzyme activity.[21]

The shape compatibility between enzymes and substrates led to the belief that organic molecules can recognize one another in the same manner. Molecular recognition is defined as the ability of a ligand (molecular receptor) to select and to bind a specific substrate out of a variety of particles.[20-22] Size and shape differences, as well as noncovalent attractive forces such as electrostatic interactions, H-bonding, and

solvophobic forces can affect the recognition of substrate (guest) molecules. For complexation to occur, binding sites and steric barriers in potential partners must be complementary to one another in electronic character and geometric arrangement.[21,22]

Organic molecules **(Figure 1.10)** that act as host molecules in complex syntheses are crown ethers (**1**), cryptands (**2**), calixarenes (**3**), and cyclodextrins (**4**). The crown ethers **1** first synthesized by Pedersen in 1967 are the most studied host molecules for complex synthesis. The shorthand notation for naming crown ethers is *n*-Crown-*m*, where *n* is the ring size (total number of atoms), and *m* is the number of oxygen atoms in the ring. There are two methods for the synthesis of crown ethers as shown in the synthesis of 18-Crown-6 (**1**) (**Scheme 1.5**).[20,23,24]

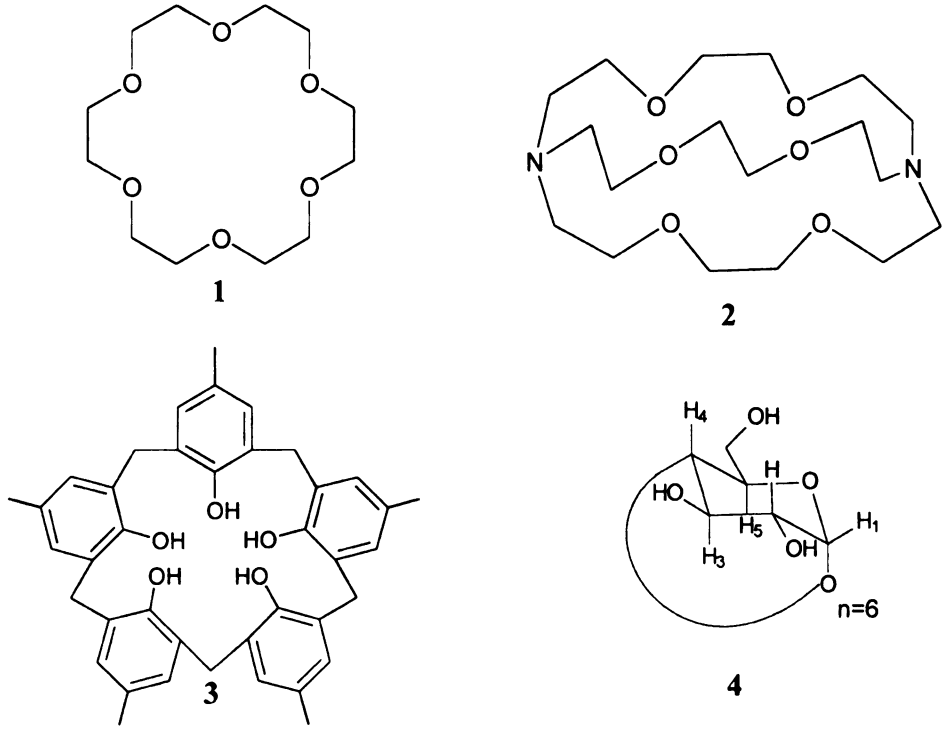

Figure 1.10. Organic host molecules.

In route A, **1** is synthesized by a nucleophile-electrophile approach, where a diol reacts with a bis(electrophile). The reaction requires a strong base to deprotonate the alcohols, and the electrophile is usually a di-chloro, bromo, or tosylated compound. In route B, a cation is used to catalyze the reaction by coordination with donor O atoms to form the cyclized polyethers. This is called the "template effect" and demonstrates the ability of crown ethers to make H-G complexes with various cations.

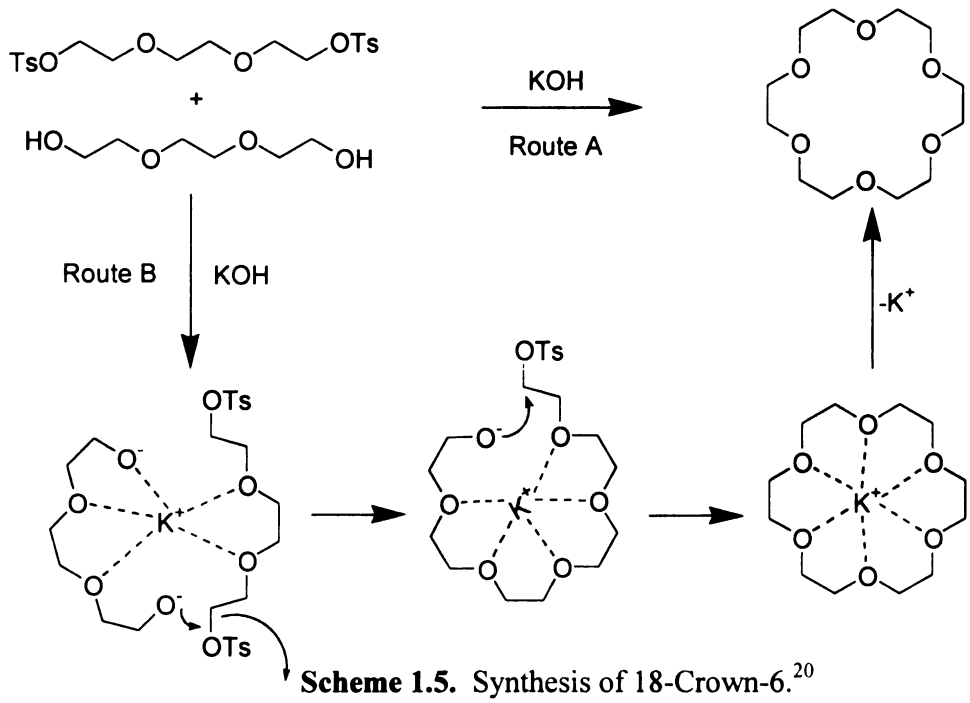

Scheme 1.5. Synthesis of 18-Crown-6.[20]

Table 1.3. Comparison of various cation and crown ether cavity diameters.[20]

Cation	Cation diameter, [Å]	Crown ether	Cation diameter, [Å]
Li^+	1.20	12-Crown-4	1.2-1.5
Na^+	1.90	15-Crown-5	1.7-2.2
K^+	2.66	18-Crown-6	2.6-2.8
Cs^+	3.38	21-Crown-7	3.4-4.3

The hydrophilic cavity of various sized crown ethers has been found to match the diameters of a wide variety of alkali, and alkaline earth metal ions (**Table 1.3**).[20,25] The complexation selectivity of crown ethers for various metal ions (and other H-G complexes) is represented by the stability constant (K_s) (**Equation 1.4**), which is equal to the rate of complex formation (k_f) divided by the rate of decomplexation (k_d). K_s is a measure of the thermodynamic stability of the complex and can be determined by changes in the physical properties of the host or guest molecule upon formation of the complex. Solubility, UV-vis spectroscopy, and shifts in ^1H and ^{13}C NMR resonances are some of the methods that have been used to determine the K_s of a H-G complex.[20,23,25]

$$\text{Host} + \text{Guest} \underset{k_d}{\overset{k_f}{\rightleftharpoons}} [\text{Host-Guest}] \qquad \textbf{Equation 1.3}$$

$$K_s = \frac{[\text{Host-Guest}]}{[\text{Host}]\,[\text{Guest}]} = \frac{(k_f)}{(k_d)} \qquad \textbf{Equation 1.4}$$

Cryptands (**2**, **Figure 1.10**) are macropolycyclic molecules that contain an intramolecular cavity of 3-dimensional shape. Cryptands are named according to the number of oxygen donor atoms that are present in the bridges.[20,21,24] Cryptand **2** has three bridges that contain two oxygen atoms in each bridge and is named as a [2.2.2] cryptand. Cryptands have enhanced stabilities over crown ethers for alkali, and alkaline earth metals as shown in **Table 1.4**.[20,23,24,26] The reason for the pronounced selectivity of cryptands for metal cations is the size complementarily between the cation and the 3-dimensional intramolecular cavity (termed "spherical recognition"), and the enhanced

number of electron pairs that contact the cation (eight heteroatoms versus six heteroatoms for 18-Crown-6).

Table 1.4. Comparison of log K_s values (in water solutions at 25 °C) of various metal cations with organic host molecules **1** and **2**.

Log K_s values of various H-G complexes in an aqueous solution				
Host	**Li^+**	**Na^+**	**K^+**	**Cs^+**
18-C-6	0	0.8	2.03	2.72
[2.2.2] Cryptand	2.0	3.9	5.4	8.0

Crown ethers and cryptands are organic host molecules that form complexes with small guests (Group 1 and other metals). These host molecules have established that structural complementarity between the guest molecule and the receptor is the key factor for accurate molecular recognition of the guest.[23] Crown ethers and cryptands have been used in various industrial applications as metal extraction agents or "scavengers".[24] The ability to recognize large macromolecules plays an essential role in the building up of supramolecular structures such as enzyme-substrate or antigen-antibody complexes, and therefore host molecules that can recognize large organic guest molecules have received much attention recently.[21,22]

Organic host molecules that can be involved in binding and recognition of small to large organic guest molecules are calixarenes and cyclodextrins (**3** and **4**, **Figure 1.10**). The name calixarene comes from the Greek work *calix*, meaning chalice (cup), and *arene* indicating the incorporation of aromatic rings in the macrocyclic array. Calixarenes are named by specifying the size of the macrocycle by a bracketed number inserted between

calix and *arene* and specifying the nature and position of substitution on the aromatic rings.[20] Calixarene **3** is named 5,11,17,23,30-pentamethyl-31,32,33,34,35-pentahydroxycalix[5]arene according to this nomenclature. Calixarenes are formed from the condensation of phenol with formaldehyde in the presence of base and usually contain 4 to 8 aromatic rings.[20,24] Calixarenes, as their name states, are cup or tub-shaped molecules, with a hydrophobic cavity that is able to incorporate organic guest molecules (**Figure 1.11**). Complexes have been made with a variety of organic guest molecules including haloforms, aromatics, nitromethane, and even C_{60} carbon fullerenes (a 1:1 complex with *p-tert*-butylcalix[8]arene). The application of calixarenes are similar to crown ethers and cryptands (as scavengers), but because calixarenes can recognize organic molecules, the applications are more numerous. Beer and Chen[27] have synthesized substituted calixarenes and incorporated them into an electrode structure for use as a sensor capable of detecting toxic vapours (PCBs) in air, while Nolan and Diamond have developed sensors that are selective for lead and mercury, as well as plutonium from nuclear wastes.[28]

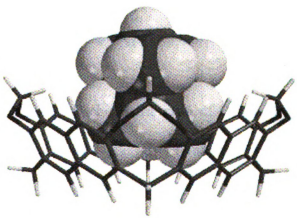

Figure 1.11. Model of a calixarene host-guest complex.

Cyclodextrin (**4**) is an example of a host molecule that is able to include large organic guest molecules. The most remarkable property of the cyclodextrins is their ability to form H-G complexes with a variety of molecules. The one condition for formation of a complex is that the guest molecule must fit entirely or at least partially into the CD cavity.[1,3,29] The properties of H-G complexes with CD are discussed in the next two sections and are directly related to the research in this manuscript.

1.3.1 Host-Guest complexes with cyclodextrin

Cyclodextrins (**Figure 1.1**) are unique host molecules because their shape (a hollow truncated cone) allows guest molecules to be included inside the cavity of the CD molecule (called an "inclusion complex" or IC).[3] CD inclusion complexes are synthesized in aqueous solutions and complex formation is driven by the attractive hydrophobic interactions involved between the interior cavity of CD and the guest molecule (**Figure 1.12**).[2] In aqueous solutions, water molecules are trapped inside the cyclodextrin cavity, which is energetically unfavorable due to polar-apolar interactions. Guest molecules that are less polar than water associate with the hydrophobic cavity of CD and release the water molecules into the bulk solution (a gain in entropy), and the complex is stabilized by Coulombic, van der Waals, or H-bonding interactions between the host and guest.[2]

ICs usually form in a 1:1 stoichiometric ratio of CD:Guest molecule, but other ratios (2:1, 1:2) have been discovered.[30] The stoichiometric ratio depends on the structure of the guest molecule, the concentration of the guest molecule in solution, as well as the solvent used for complex formation. ICs are isolated as a stable crystalline

substance, but in solution an equilibrium is established between the complexed species and the decomplexed species (represented by **Equations 1.3** and **1.4**).

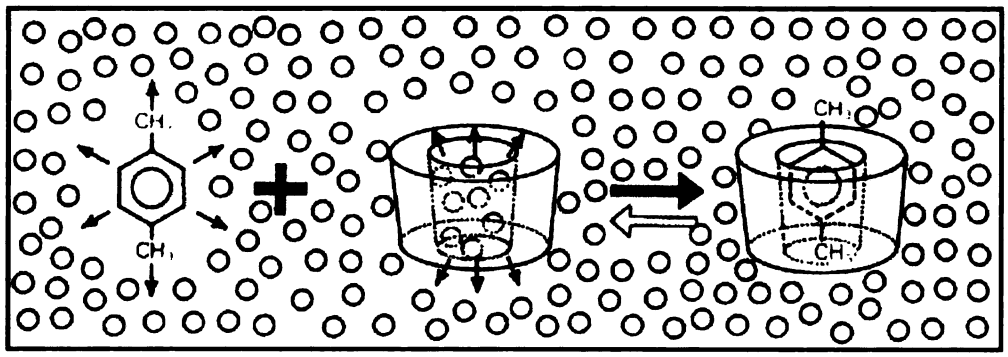

Figure 1.12. A schematic representation of CD inclusion complex formation with *p*-xylene as the guest molecule.[2] In this illustration by Szejtli, the small circles represent water molecules.

In the formation of ICs, guest molecules are arranged in the crystal lattice in either a channel or caged structure.[31,32] The solid-state crystal structure of α-CD hydrate is shown in **Figure 1.13**, and is an example of a cage-type crystal structure.[32] There are two types of cage structures that exist for CD inclusion complexes: herringbone and brick-type **(Figure 1.14)**. Research by Saenger[29-31,33] and Harata[32] have shown that depending on the size and structure of the guest molecules, different crystal structures are formed. The crystal structure of α-CD hydrate is an example of the herringbone cage-type crystal structure. In this crystal structure CDs are packed crosswise so that the interior cavity of CD is blocked on both sides by other CD molecules. Herringbone crystal structures occur in CD complexes when the guest is a small molecule such as methanol or propanol. Because small guest molecules are included inside the cavity of CD and don't extend beyond the dimensions of the CD cavity, the inclusion complex crystal structure resembles that of uncomplexed CD (**Figure 1.13**). Brick-type cage structures **(b, Figure 1.14[32])** are produced from complexes with para-disubstituted

benzenes. The crystal packing is reminiscent of the offset layering of bricks in a wall, where layers of CD molecules above and below block individual CD cavities. Harata discovered that the more polar groups of a number of 1,4-substituted aromatic compounds are located near the wide rim of the CD torus (2° OH groups), while nonpolar groups are directly inserted through the CD cavity (near narrow rim, 1° OH groups).[32] Besides *p*-disubstituted aromatic compounds, α-CD complexes with N,N-dimethylformamide, and 2-pyrrolidone have been discovered to have a layered type of crystal structure.[32] The space group for both the herringbone and brick-caged crystal structure is D_{2h} and orthorhombic. The unit cell is primitive (P) and is defined as $P2_12_12_1$ by the International Tables of X-ray Crystallography.

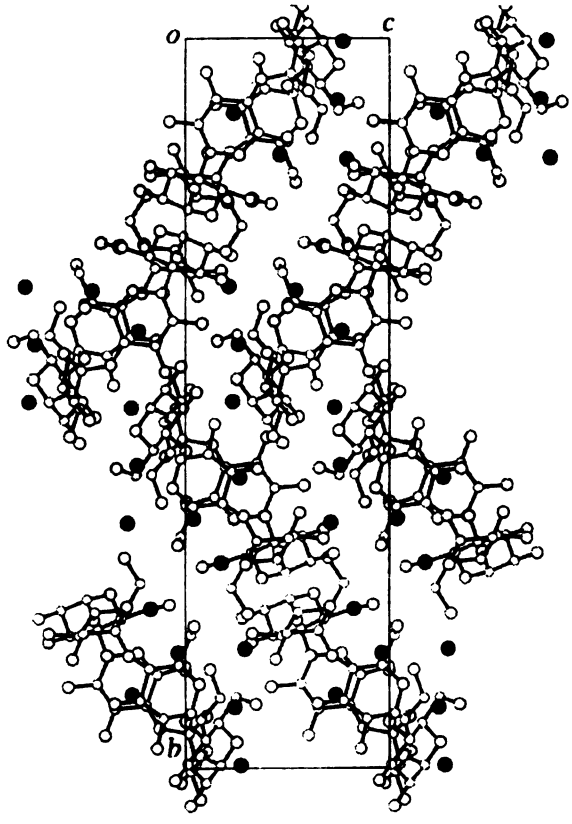

Figure 1.13. X-ray crystal structure of α-CD hexahydrate viewed along the *a* axis.[32] Dark circles represent water molecules in the crystal structure.

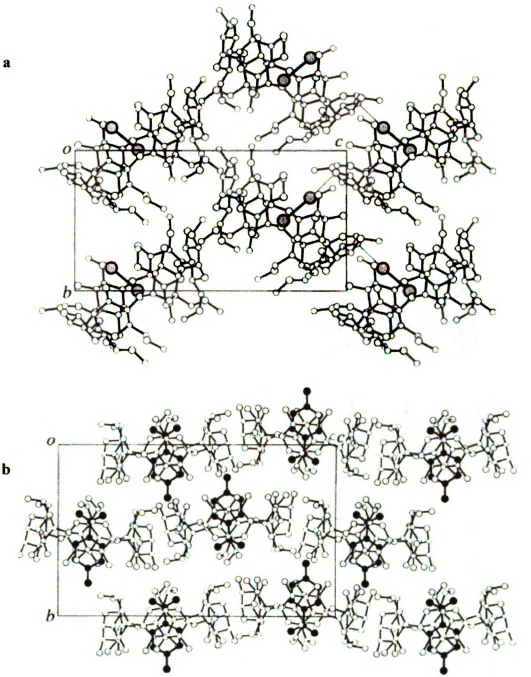

Figure 1.14. Crystal structures of (a) dimethyl-α-CD complexed with iodine (herringbone-type cage) and (b) α-CD complexed with *p*-nitrophenol (brick-type cage).[32] Both crystal structures are viewed along the *a* axis.

As was shown in the cage-type crystal structure, the crystal structure (herringbone or brick) is dependent on the structure and size of the guest, which is also true in distinguishing between channel-type and cage-type crystal structures. Small molecular guests (< 5 carbon atoms in a straight chain) crystallize in cage structures whereas organic guest molecules larger than five carbon atoms long, form channel-type crystal structures.[30,32] In channel-type complexes **(Figure 1.15)**, CDs are stacked head-to-tail or head-to-head to form columnar crystals in which the guest molecules are embedded inside the cavity of CD.

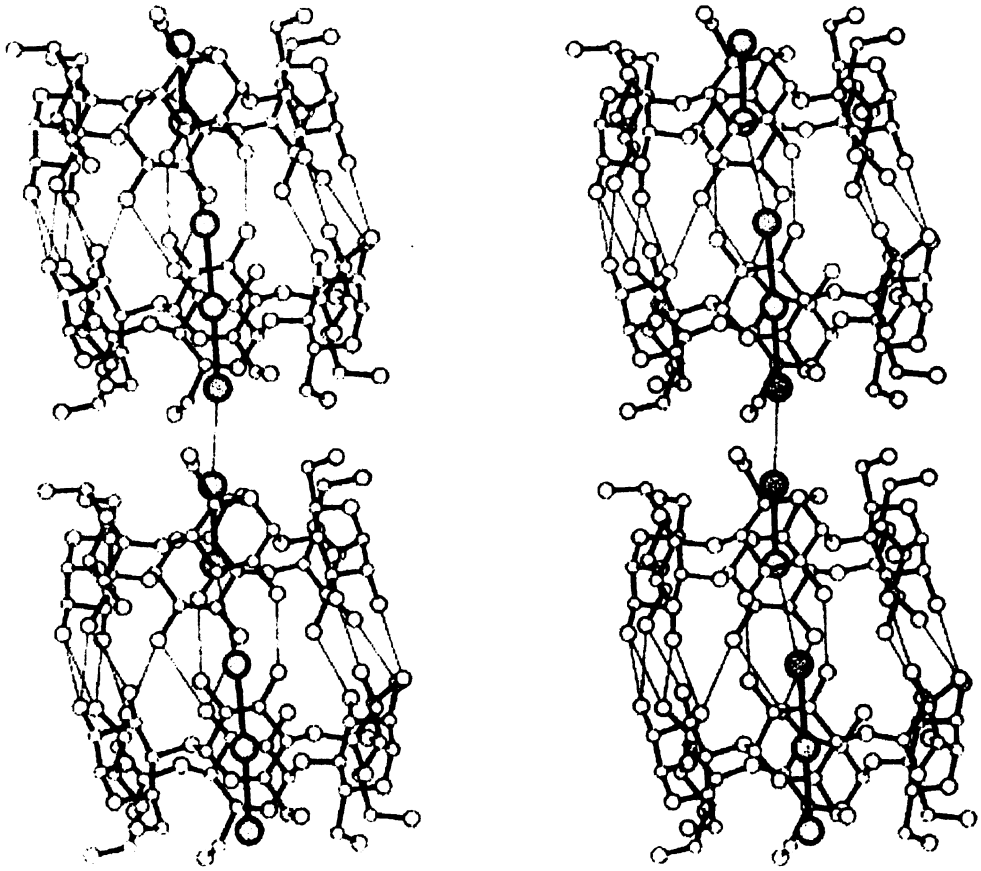

Figure 1.15. Stereodrawing of the structure of α-CD complexed with an iodine-iodide lithium salt (channel-type crystal structure).[32]

X-ray crystal structures of inclusion complexes provide important information on the three-dimensional structure of H-G complexes as well as information on the noncovalent interactions involved in complex formation. The importance of this knowledge has led to the interest in synthesizing other inclusion complexes with CD. The relative ease of complex formation is also responsible for the explosion in the number of CD inclusion complexes. The belief that CD can recognize differences in organic molecules has drawn attention to the use of CD for the self-assembly of nanoscale structures. Molecular machines, sensors, and artificial receptors are some of the proposed uses for these nanoscale structures. Cyclodextrin is also able to form H-G complexes with macromolecular compounds (polymers) and the properties of these complexes are discussed in the next section.

1.3.2 Polymeric inclusion complexes

Since the development of host/guest chemistry scientists began to look at Nature for their next inspirations in the development of supramolecular complexes (association of two or more chemical species held together by intermolecular forces).[21,22] Dendrimers and C_{60} (fullerene) are some examples of chemical species that mimic those structures found in Nature or architectural design.[34] Interlocked and intertwined structures are examples of supramolecular complexes that have gained much interest not only for their beauty but also because of their possible applications as nanoscale machines.

When an acyclic molecule is inserted inside the cavity of a macrocyclic molecule the supramolecular complex is termed a pseudorotaxane (**I, Figure 1.16**).[34-37] Pseudorotaxanes are in equilibrium with their uncomplexed state. The attachment of bulky groups to the ends of the acyclic molecule prevents dissociation into its free

components. Such molecules are termed rotaxanes (**II, Figure 1.16**), from the Latin *rota* meaning wheel, and *axis* meaning axle.

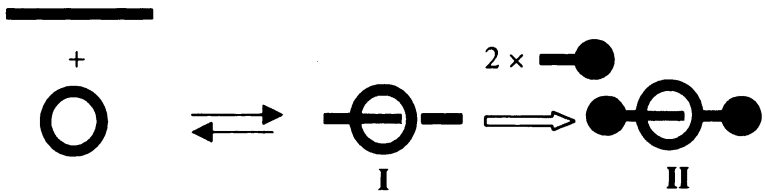

Figure 1.16. Diagram of the reversible formation of a pseudorotaxane (**I**) from its acyclic and cyclic components, and the irreversible conversion into a rotaxane (**II**).

Pseudorotaxanes form by threading the macrocycle onto the acyclic polymer chain in aqueous solutions. The free and bound states of these mechanically interlocked complexes have different physical properties, which has led to studying these compounds as models for self-assembly in nanoscale structures. The driving force for the formation of these supramolecules are noncovalent attractive forces (which are found to be responsible for the formation of highly organized biological systems such as membranes and ribososmes), so these molecules can be used as models for the investigation of complex biological entities.[3]

Since the early 1990's it has been known that cyclodextrins thread onto polymer chains to form supramolecular inclusion complexes such as polypseudorotaxanes (**III**) and polyrotaxanes (**IV**).[3,35-37] In these structures many CDs are located on the polymer backbone structure to form a type of molecular abacus.

III **IV**

Figure 1.17. Diagrams of polypseudorotaxanes (**III**) and polyrotaxanes (**IV**).

Harada *et al.* was the first to report the complex formation between CD and a polymer, an IC formed from α-CD and poly(ethylene glycol) (PEG).[38,39] The complex formed upon the addition of PEG to a saturated aqueous solution of α-CD. After stirring the solution overnight, Harada *et al.* collected a white solid precipitate (inclusion complex) by filtration. Numerous experiments were performed on the synthesized inclusion complexes to confirm their composition and properties. ^{1}H NMR showed a 2:1 ratio of the proton resonances from α-CD and PEG, corresponding to a stoichiometry of two ethylene glycol units per α-CD. X-ray powder diffraction of the complexes shows that they are crystalline and the patterns correspond to a column or channel crystal structure. ^{13}C CP/MAS NMR also confirmed that a polymer chain was threaded through the CD cavity. **Figure 1.18** is a proposed model by Harada[36] showing the complex formed between α-CD and PEG. Harada has also observed that complex formation was selective with only α-CD forming a complex with PEG. β-CD did not form a complex with PEG because its interior cavity is too large to establish strong interactions with the acyclic polymer. Harada has since made inclusion complexes with various polymers including poly(isobutylene)[40] (PIB), poly(ε-caprolactone)[41] (PCL), and most recently poly(dimethylsiloxane).[42]

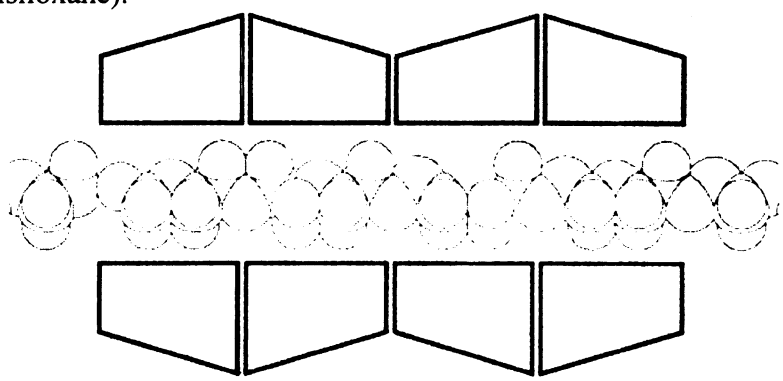

Figure 1.18 Proposed superstructure for PEG-α-CD complexes as illustrated by Harada.[36]

The combination of CD's affinity to bind almost an infinite number of guest molecules with its ability to form self-assembled supramolecular structures has provided numerous research possibilities and industrial applications. Recently Hayakawa *et al.*[43] synthesized nanotubes consisting of CD molecules. Nanotubes are fine capillaries with an inside diameter of nm order which have attracted great interest for their use as sites for molecular recognition. The nanotube was prepared by threading CD onto a polymer chain (PEG-BA) with bulky ends to form a polyrotaxane. A molecular tube was then formed by cross-linking adjacent CD units in the polyrotaxane structure, and when the bulky end groups were removed, the nanotube unthreaded from the polymer chain. The synthesized nanotube was studied as a host for the reversible binding of small molecules such as iodine.

The synthesis of supramolecular structures that contain molecularly imprinted polymers is another example where the complexing ability of CDs is used. Komiyama *et al.*[44] designed polymeric receptors for cholesterol by crosslinking β-CD with diisocyanates in the presence of cholesterol as a template. Initial studies showed that 70% of the cholesterol in a water-THF mixture was absorbed by the templated polymer receptor. Nicholls *et al.*[45] developed a method to synthesize synthetic receptors for water-soluble substances. In Nicholls' approach, β-CD was used as the receptor for effective recognition of D and L-phenylalanine in aqueous solutions.

The above examples show the versatility of polymer inclusion complexes with CD. The understanding of the interactions involved in the self-assembly of supramolecular structures is important for the efficient design and recognition of guest molecules. The research presented in this thesis gives information on the ability of CD to

form complexes with a series of amphiphilic $(AB)_n$ block copolymers. Possible molecular recognition of CD for one of the polymer blocks, as well as changes in the physical properties of both reactants are discussed.

1.4 References

(1) Bender, M., Komiyama, M. *Cyclodextrin Chemistry*; Springer-Verlag: New York, 1978.

(2) Szejtli, J. *Chemical Reviews* **1998**, *98*, 1743-1753.

(3) Wenz, G. *Angewandte Chemie-International Edition in English* **1994**, *33*, 803-822.

(4) Hedges, A. R. *Chemical Reviews* **1998**, *98*, 2035-2044.

(5) Odian, G. *Principles of Polymerization.* 2nd Ed.; John Wiley & Sons: New York, 1981.

(6) Stroble, G. R. *The Physics of Polymers: Concepts for Understanding Their Structures and Behavior*; 2nd ed.; Springer-Verlag: New York, **1997**.

(7) Seymour, R. B.; Carraher, C. E., Jr. *Polymer Chemistry. An Introduction.*; Marcel Dekker: New York, 1981.

(8) Porter, M. R. *Handbook of Surfactants*, 1st Ed.; Chapman and Hall: New York, 1991.

(9) Nace, V. M.; Editor *Nonionic Surfactants: Polyoxyalkylene Block Copolymers.*; Marcel Dekker, Inc.: New York, 1996.

(10) Alexandridis, P.; Lindman, B.; Editors *Amphiphilic Block Copolymers: Self-Assembly and Applications.*; Elsevier Science: Amsterdam, 2000.

(11) Qiao, J.; Chen, Y. Y.; Baker, G. L. *Chemistry of Materials* **1999**, *11*, 2542-2547.

(12) Chen, Y. Y.; Ph.D. Dissertation. Michigan State University, 1999.

(13) Swan, K. A.; Stowe, M. K.; Chen, Y.; Qiao, J.; Baker, G. L. *Polymer Preprints* **2000**, *41*(2), 1365.

(14) Wagener, K. B.; Boncella, J. M.; Nel, J. G. *Macromolecules* **1991**, *24*, 2649-57.

(15) Schwab, P.; Grubbs, R. H.; Ziller, J. W. *Journal of the American Chemical Society* **1996**, *118*, 100-10.

(16) Schrock, R. R.; Murdzek, J. S.; Bazan, G. C.; Robbins, J.; DiMare, M.; O'Regan, M. *Journal of the American Chemical Society* **1990**, *112*, 3875-86.

(17) Chen, Y. Y.; Baker, G. L. *Journal of Organic Chemistry* **1999**, *64*, 6870-6873.

(18) Chen, Y. Y.; Baker, G. L.; Ding, Y. Q.; Rabolt, J. F. *Journal of the American Chemical Society* **1999**, *121*, 6962-6963.

(19) Keegstra, E. D.; Zwikker J. W.; Roest, M. R.; Jenneskens, L. W. *Journal of Organic Chemistry* **1992**, *57*, 6678-6680.

(20) *Host Guest Complex Chemistry: Macrocycles: Synthesis, Structures, Applications*; Vogtle, F. W., E, Ed.; Springer-Verlag: New York, 1985.

(21) *Supramolecular Chemistry: Concepts and Perspectives*; Lehn, J.-M., Editor.; VCH Publishers: New York, 1995.

(22) Tsoucaris, G.; Editor *Current Challenges on Large Supramolecular Assemblies.*; Kluwer Academic Publishers: Boston, 1999.

(23) *Crown Compounds: Toward Future Applications*; Cooper, S. R., Editor.; VCH Publishers: New York, 1992.

(24) Constable, E. C. *Coordination Chemistry of Macrocyclic Compounds.*; Oxford University Press: New York, 1999.

(25) *Crown Ethers and Analogous Compounds*; Hiraoka, M., Ed.; Elsevier Science: New York, 1992; Vol. 45.

(26) *Crown Ethers and Analogs*; Patai, S. R., Zvi, Editors.; John Wiley & Sons: New York, 1989.

(27) Beer, P.; Shade, M.; Chen, Z.; *PCT International Applications*: Patent No. WO9511449, 1995.

(28) Diamond, D.; Nolan, K. *Analytical Chemistry* **2001**, *73*, 22A-29A.

(29) Saenger, W. *Angewandte Chemie-International Edition in English* **1980**, *19*, 344-362.

(30) Saenger, W.; Steiner, T. *Acta Crystallographica Section A* **1998**, *54*, 798-805.

(31) Saenger, W. R.; Jacob, J.; Gessler, K.; Steiner, T.; Hoffmann, D.; Sanbe, H.; Koizumi, K.; Smith, S. M.; Takaha, T. *Chemical Reviews* **1998**, *98*, 1787-1802.

(32) Harata, K. *Chemical Reviews* **1998**, *98*, 1803-1827.

(33) Saenger, W.; McMullan, R. K.; Fayos, J.; Mootz, D. *Acta Crystallography, Sect. B* **1974**, *B30*, 2019-28.

(34) Amabilino, D. B.; Stoddart, J. F. *Chemical Reviews* **1995**, *95*, 2725-829.

(35) Philp, D.; Stoddart, J. F. *Angewandte Chemie-International Edition in English* **1996**, *35*, 1155-1196.

(36) Nepogodiev, S. A.; Stoddart, J. F. *Chemical Reviews* **1998**, *98*, 1959-1976.

(37) Raymo, F. M.; Stoddart, J. F. *Chemical Reviews* **1999**, *99*, 1643-1663.

(38) Harada, A.; Kamachi, M. *Macromolecules* **1990**, *23*, 2821-2823.

(39) Harada, A.; Li, J.; Kamachi, M. *Macromolecules* **1993**, *26*, 5698-5703.

(40) Harada, A.; Suzuki, S.; Okada, M.; Kamachi, M. *Macromolecules* **1996**, *29*, 5611-5614.

(41) Kawaguchi, Y.; Nishiyama, T.; Okada, M.; Kamachi, M.; Harada, A. *Macromolecules* **2000**, *33*, 4472-4477.

(42) Okumura, H.; Okada, M.; Kawaguchi, Y.; Harada, A. *Macromolecules* **2000**, *33*, 4297-4298.

(43) Ikeda, E.; Okumura, Y.; Shimomura, T.; Ito, K.; Hayakawa, R. *Journal of Chemical Physics* **2000**, *112*, 4321-4325.

(44) Asanuma, H.; Kakazu, M.; Shibata, M.; Hishiya, T.; Komiyama, M. *Chemical Communications* **1997**, 1971-1972.

(45) Piletsky, S. A.; Andersson, H. S.; Nicholls, I. A. *Macromolecules* **1999**, *32*, 633-636.

CHAPTER 2

Synthesis and Characterization of Inclusion Complexes of α-CD and $(AB)_n$ Block Copolymers

2.1 Acronyms for compounds used in this research

The polymers and triblock oligomers used in this research contain two segments, an ethylene oxide chain and either an *n*-alkyl or an *n*-alkyl chain that contains a single double bond. For simplicity, the nomenclature system used to refer to these compounds is similar to that of PEO/PE surfactants. $(AB)_n$ block copolymers are abbreviated as $[C_x\pi C_xEO_y]_n$, where C_x corresponds to x methylene units, π represents the two carbon atoms of the double bond, and EO_y refers to y ethylene oxide repeat units. ABA triblock oligomers are abbreviated as $C_xEO_yC_x$ and follow the same scheme used to represent the block copolymers. α-Cyclodextrin is abbreviated as α-CD. Inclusion complexes (ICs) with $(AB)_n$ block copolymers and ABA triblock oligomers are abbreviated as $(AB)_n$-α-CD or ABA-α-CD ICs respectively. Specific polymer or triblock oligomer inclusion complexes use the surfactant nomenclature along with α-CD. Examples of the naming protocol are shown in **Scheme 2.1**.

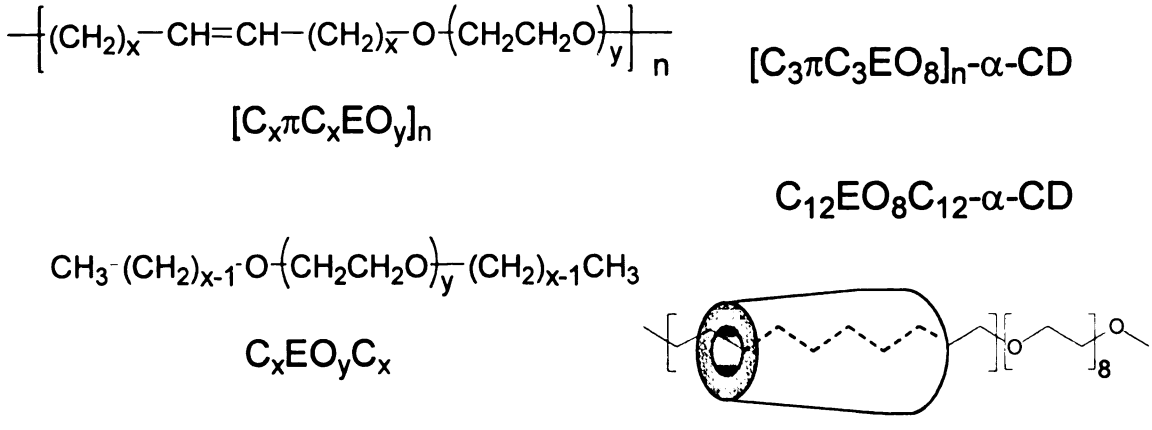

Scheme 2.1. Nomenclature of $(AB)_n$ block copolymers, ABA model compounds, and inclusion complexes formed with α-CD. A proposed structure of a $(AB)_n$-α-CD complex is also shown.

2.2 Results

2.2.1 Complex formation between $[C_x\pi C_xEO_y]_n$ polymers and α-CD.

Inclusion complexes of α-CD and $[C_x\pi C_xEO_y]_n$ polymers were prepared at room temperature by adding 2 mL of a 20 wt% solution of α-CD in water to a solution of the $(AB)_n$ block copolymer in 0.5 mL methanol. Inclusion complexes were synthesized at various polymer concentrations to determine the stoichiometry of the complexes (see below). For these experiments, polymer concentrations (2-40 mg/mL) were calculated by dividing the weight of the polymer sample (in milligrams) by the total volume of solution (water + methanol = 2.5 mLs). For low polymer concentrations (< 8 mg/mL), the α-CD and polymer solutions became turbid on mixing, and the complex precipitated as white crystals which were collected by filtration and washed with water to remove uncomplexed α-CD. Uncomplexed polymer formed a milky suspension that passed through the filter paper, and a control experiment run in the absence of α-CD showed that 98% of the polymer could be recovered from the filtrate. Thus, the polymer/α-CD complexes reported here are not contaminated by free polymer. All complexes were dried overnight in a vacuum oven (150°C) to remove residual water from the complex. Higher polymer concentrations (> 12 mg/mL) led to formation of a white gel, which was washed to remove uncomplexed polymer and α-CD and isolated as a crystalline IC by freeze-drying. The gel formed more rapidly at higher polymer concentrations. Our observations are in agreement with those of Baglioni *et al.*, who reported the formation of white solid gels during the synthesis of ICs from α-CD and PEG in aqueous solutions.[1,2] He also described the threading process for the formation of these complexes, and the effects that temperature and composition have on complex formation. **Table 2.1** lists the

$(AB)_n$ block copolymers that were used in the synthesis of ICs with α-CD. The characteristics of the syntheses of ICs from α-CD and $[C_x\pi C_xEO_y]_n$ polymers were all similar in their formation.

Table 2.1 Characteristics of $(AB)_n$ block copolymers used in IC formation with α-CD.

$(AB)_n$ block copolymer	**M_n[1](g/mol)**	**Concentrations of polymer (mg/mL) in solution**
$[C_3\pi C_3EO_6]_n$	25,000	2, 4, 8, 12, and 16
$[C_3\pi C_3EO_7]_n$	26,000	2, 4, 8, 12, 16, and 20
$[C_3\pi C_3EO_8]_n$	47,000	2, 4, 8, 10, 12, 16, 20, 24, and 40
$[C_4\pi C_4EO_8]_n$	19,000	2, 4, 8, 10, 12, 16, 20, 24, and 40

[1] Molecular weight data for $(AB)_n$ polymers was obtained by Chen.[3]

The yield of the $[C_x\pi C_xEO_y]_n$-α-CD ICs, defined as (mass of the isolated complex)/(mass of α-CD + mass of polymer) are shown in **Figure 2.1.** The yields increase linearly with the concentration of polymer used in the synthesis, and saturation of the yield was observed in all cases. The yields of complexes at different concentrations were repeatable within 2%. The saturation point corresponds to the polymer concentrations where gelation of the polymer-CD solution was observed, (generally > 12 mg/mL), and depends on the chemical structure of the $(AB)_n$ polymer. Similar saturation effects were seen during the synthesis of inclusion complexes between α-CD and PEO[4] and PCL.[5] The explanation given for saturation of the yield is that the complexes have a characteristic stoichiometry in terms of the number of CDs threaded per polymer repeat unit. In ICs with PEO, one α-CD molecule is threaded for every two ethylene oxide units, while PCL-α-CD complexes have a 1:1 stoichiometry. The

stoichiometry of $(AB)_n$-α-CD ICs was determined by two different methods and is discussed in the next section.

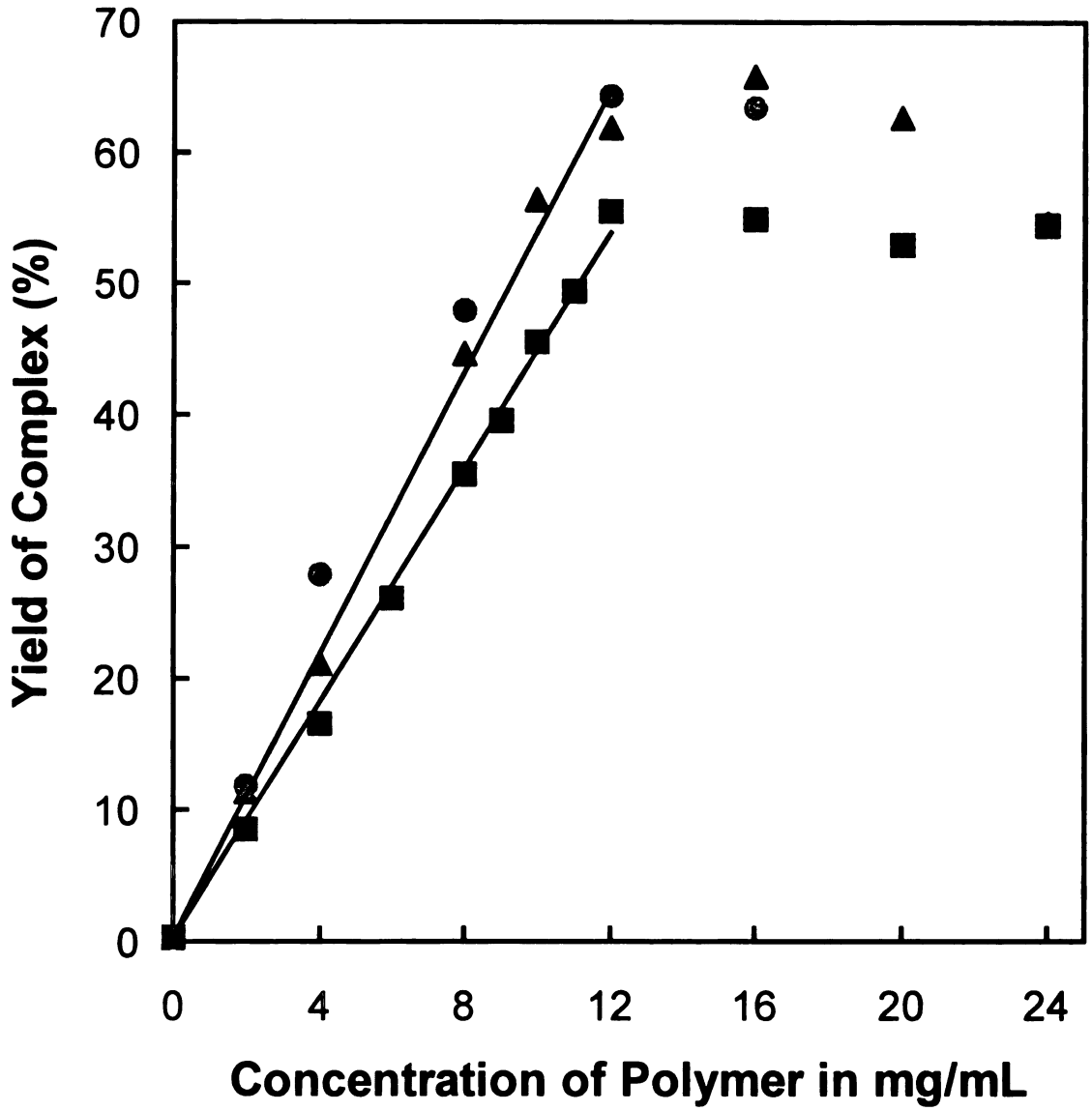

Figure 2.1. Yield of $[C_x\pi C_xEO_y]_n$-α-CD inclusion complexes as a function of polymer concentration. (■ $[C_3\pi C_3EO_8]_n$-α-CD, ▲ $[C_4\pi C_4EO_8]_n$-α-CD, ● $[C_3\pi C_3EO_6]_n$-α-CD).

2.2.2 Properties of $(AB)_n$-α-CD complexes

1) Thermal behavior

Thermal analysis was used to confirm formation of $(AB)_n$-α-CDs complexes. Representative Differential Scanning Calorimetry (DSC) and Thermal Gravimetric Analysis (TGA) data for α-CD, $[C_x\pi C_xEO_y]_n$, and the $[C_x\pi C_xEO_y]_n$-α-CD ICs are shown in **Figures 2.2** and **2.3-2.4** respectively. The data for complexes synthesized from the other polymers are similar. These results are similar to those observed by Harada and Tonelli who have synthesized ICs with α-CD and PEG.[1,6-8] **Figure 2.2** shows DSC scans for the polymer $[C_3\pi C_3EO_6]_n$ (bottom trace), and the $[C_3\pi C_3EO_6]_n$-α-CD inclusion complex (top trace). All samples were heated to 150°C to erase their thermal history and flash-cooled to −100°C. The scans shown are the second heating scans, run at 10°C/min. under He, and normalized with respect to sample mass. The DSC scan of the pure polymer has a well-defined T_g as well as a complicated sequence of exo and endotherms associated with crystalline transitions in the polymer. These transitions are barely visible in the scan of the IC, indicating that the amount of free polymer in the complex is small. Integration of the melting transition leads to an estimate of about 10% free polymer in the sample. Integration of the initial heating scan (from 25 to 150°C) indicates only 1-2% free polymer in the complex sample, and thus most of the free polymer seen in the second scan must result from partial dethreading during the scan used to erase the thermal history. As a control, we de-threaded an IC by stirring the complex in THF. The solution was filtered to remove the insoluble α-CD, concentrated, and dried under vacuum. The DSC scan of the dethreaded product shows the characteristic melting and crystallization peaks of the free polymer.

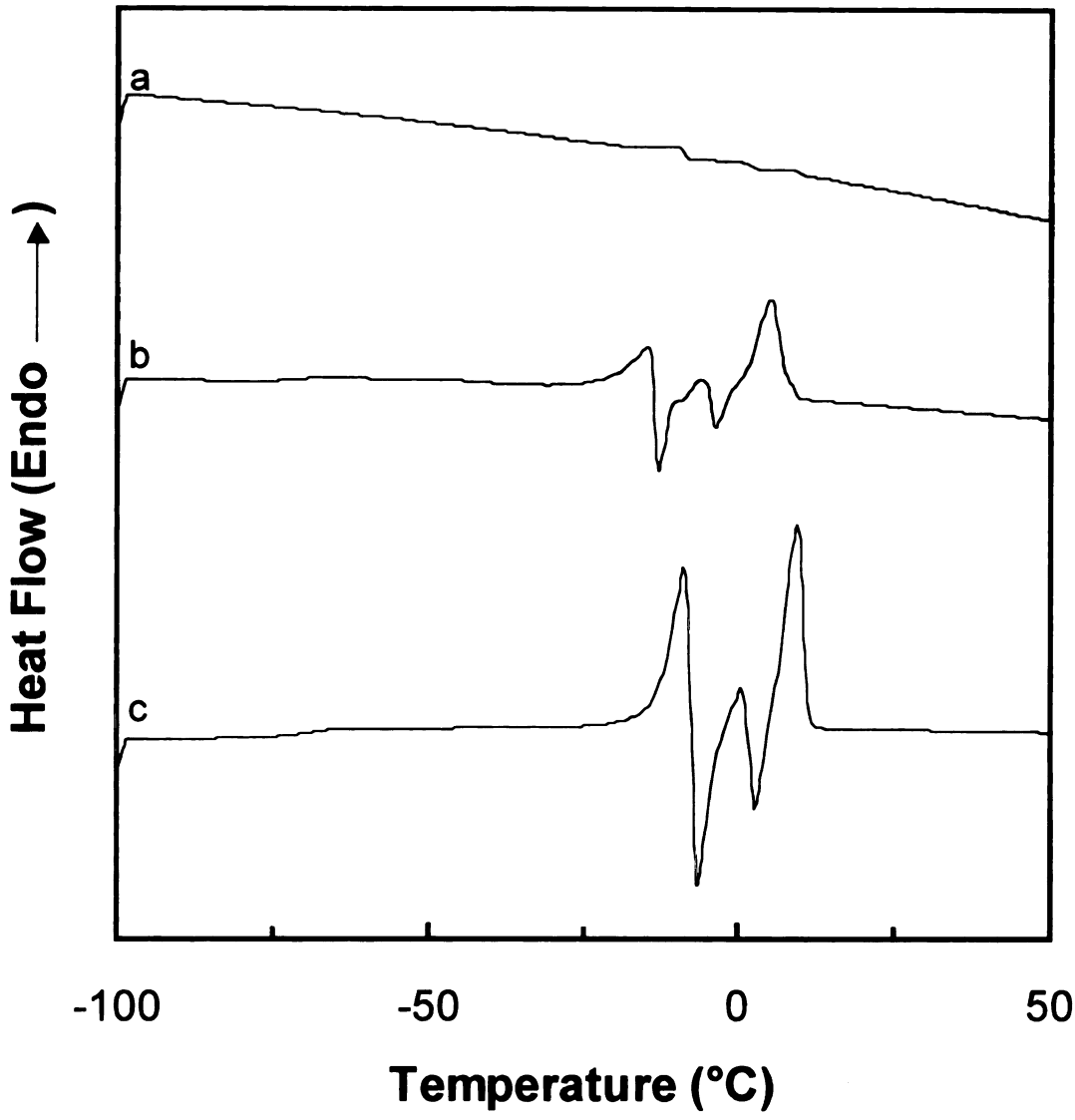

Figure 2.2. Normalized DSC thermograms of a) $[C_3\pi C_3EO_6]_n$-α-CD IC, b) the de-threaded complex and c) the pure $[C_3\pi C_3EO_6]_n$ homopolymer. All scans were run at 10°C/min under helium.

Shown in **Figure 2.3** are TGA data for α-CD, $[C_4\pi C_4EO_8]_n$, and the $[C_4\pi C_4EO_8]_n$-α-CD IC. α-CD shows an onset for weight loss at 310°C, while the polymer (trace a) has an onset for weight loss at 360°C. Both α-CD and the polymer show small residues. The TGA data for the $[C_4\pi C_4EO_8]_n$-α-CD IC is more complex. The onset for decomposition is 340°C, between that of α-CD and the pure polymer, and the decomposition profile shows a rapid weight loss to ~25% of the original weight, followed by completion of the decomposition process at a higher temperature. Because the DSC results imply that the ICs contain little free polymer, we surmise that the second step in the TGA curve for the polymer-CD IC results from dethreading of the IC during the TGA run.

For controls, physical mixtures of α-CD and $(AB)_n$ polymers were also characterized by TGA and DSC. The TGA data for a physical mixture of $[C_3\pi C_3EO_6]_n$ and α-CD (trace c in **Figure 2.4**) show a different decomposition profile than that of the synthesized $[C_3\pi C_3EO_6]_n$-α-CD IC. The TGA scan of the mixture clearly shows two distinct decomposition profiles associated with CD and the $(AB)_n$ block copolymer. The inclusion complex's profile shows an increase in the onset for decomposition over α-CD and the physical mixture. The DSC data of a physical mixture of α-CD and $[C_3\pi C_3EO_7]_n$ (data not shown) has barely observable thermal transitions associated with the free polymer, and look like previous scans of synthesized inclusion complexes (**Figure 2.2**, trace a). Although the DSC scans of synthesized $(AB)_n$-α-CD ICs look similar to a physical mixture of the two components, the dethreading experiment proves complex formation occurs and the thermal properties of ICs are quite different than their individual components.

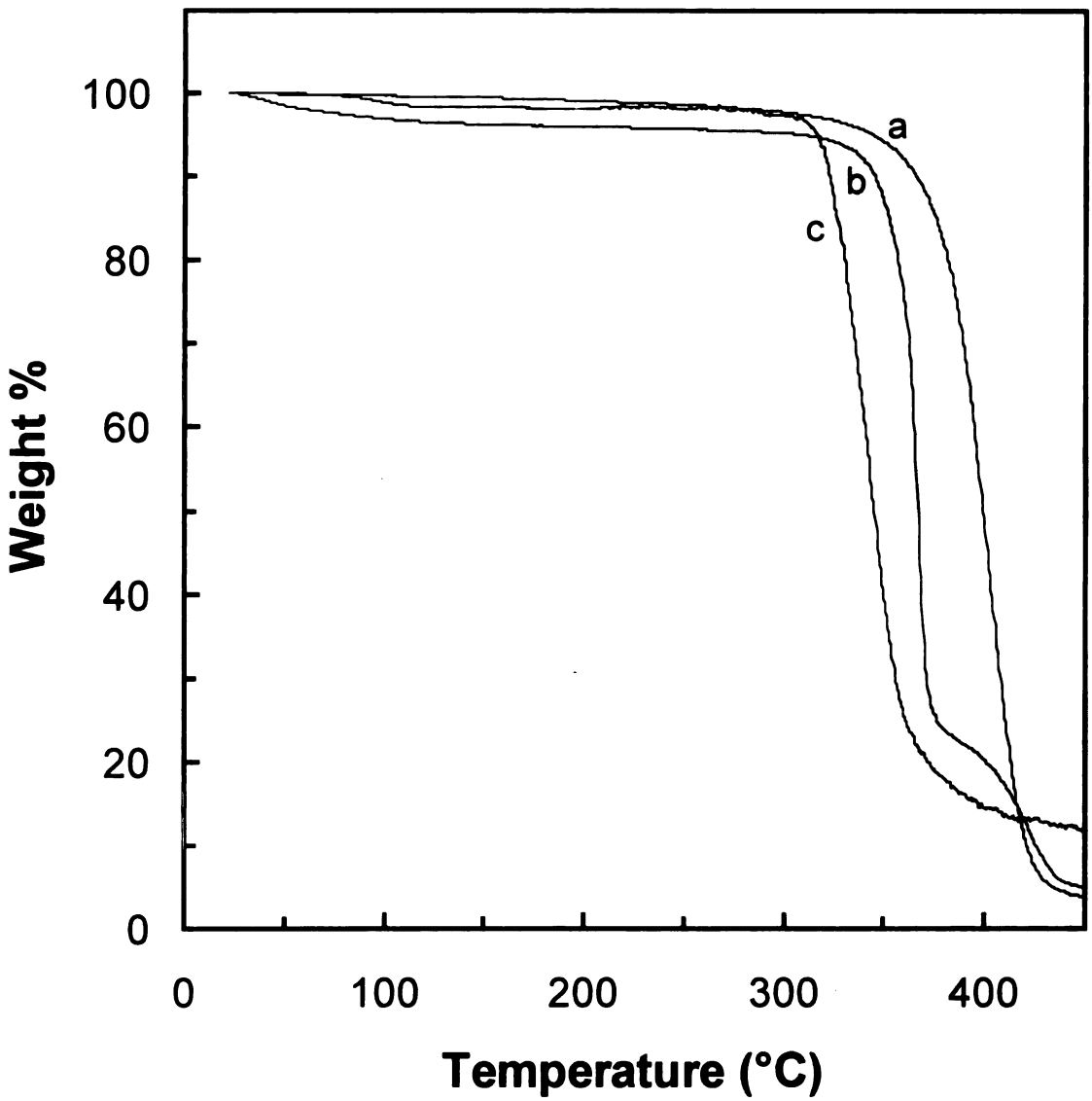

Figure 2.3. TGA scans for a) $[C_4\pi C_4EO_8]_n$, b) $[C_4\pi C_4EO_8]_n$-α-CD IC, and c) α-CD (the sample was dried for 12 h at 100°C at the beginning of the run.) Samples were heated at 10°C/min. under a flow of nitrogen.

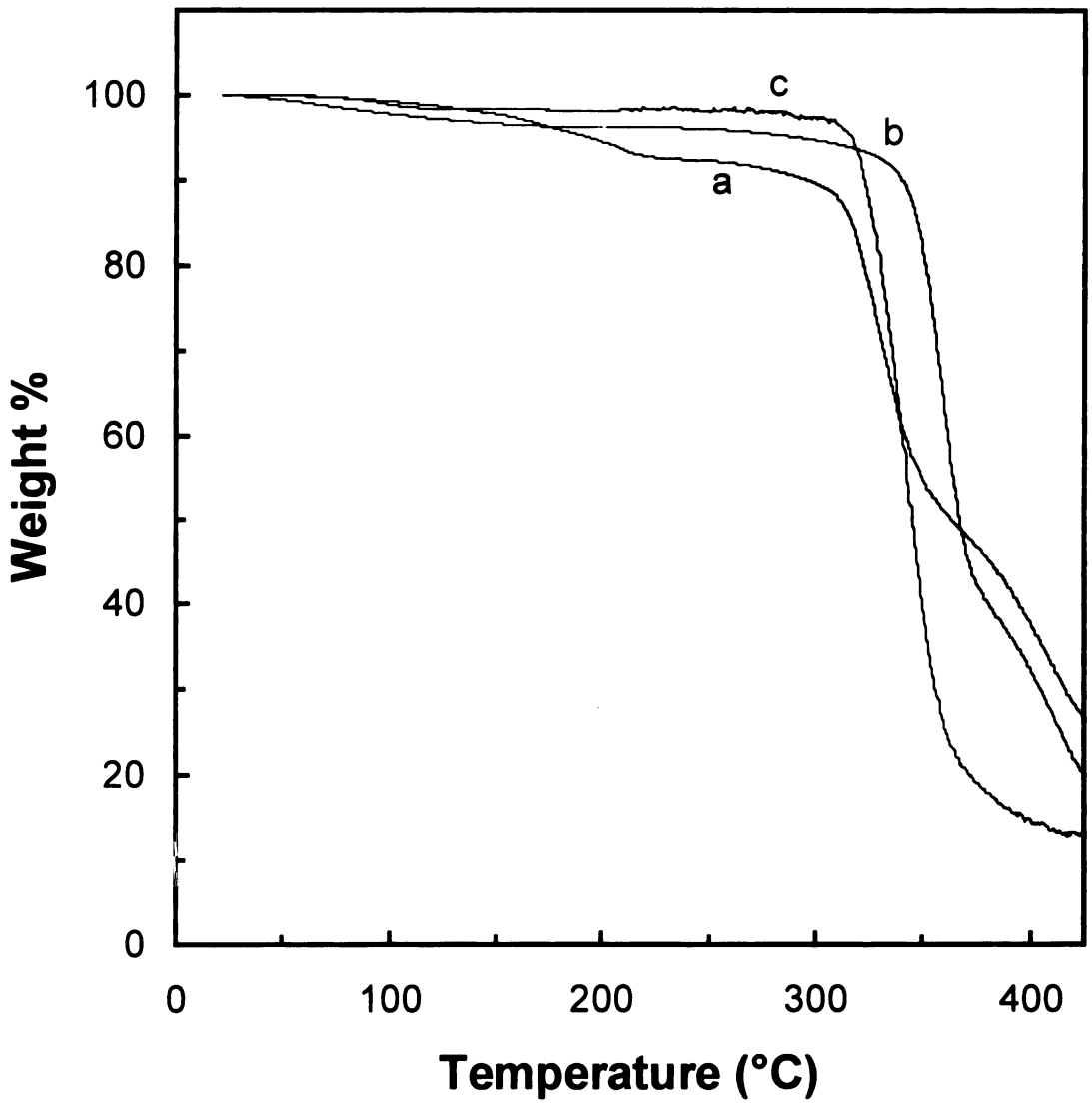

Figure 2.4. TGA scans for a) $[C_3\pi C_3EO_6]_n$ + α-CD mixture, b) $[C_3\pi C_3EO_6]_n$-α-CD IC, and c) α-CD. Samples were heated at 10°C/min. under a flow of nitrogen.

2) Solid state properties of ICs

Powder x-ray diffraction and solid-state ^{13}C CP/MAS NMR was used to determine the structure of the inclusion complexes as well as confirm complex formation. Diffraction data from inclusion complexes with known crystal structures were compared with those from $(AB)_n$-α-CD ICs. The propanol-α-CD and octanol-α-CD inclusion complexes[9-12] are known to have caged (herringbone) and column (channel) crystal structures respectively, and the XRD patterns of these complexes were used to identify the structures of the $(AB)_n$-α-CD inclusion complexes. **Figure 2.5** shows the x-ray powder patterns for a) the propanol-α-CD complex, b) $[C_3\pi C_3EO_6]_n$-α-CD, c) $C_{14}EO_8C_{14}$-α-CD, and d) the octanol-α-CD IC. The packing of the propanol-α-CD caged type crystal structure is orthorhombic with space group $P2_12_12_1$ (similar to crystal structure of α-CD hexahydrate, **Figure 1.13**).[13] The cell dimensions are: a = 14.292 Å, b = 37.515 Å, c = 9.393 Å. The octanol-α-CD IC shows the x-ray diffraction pattern associated with the channel type crystal structure of α-CD guest molecules. The channels are packed in a hexagonal unit cell and show characteristic Bragg diffraction peaks at 1, $\sqrt{3}$, and $\sqrt{7}$ corresponding to 2θ = 7.45°, 12.97°, 19.94°, and 22.65°. These peaks have been assigned to be 100, 110, and 210 reflections by Topchieva in PEG-α-CD ICs.[6,7,14-17] The prominent peak at 20.0° (210 reflection) has been reported to be diagnostic for the formation of an inclusion compound inside the channel of the CD. A comparison of the diffraction patterns of the known inclusion complexes (octanol and propanol-α-CD) shows that the $(AB)_n$ ICs are crystalline and are consistent with a columnar structure. These results are similar to the crystal structure of other polymeric inclusion complexes (PCL, PIB, and PDXL)[5,16,18-20] with cyclodextrin. Recently, Ripmeester and coworkers

obtained a single crystal X-ray structure of PEG-β-CD IC.[21] The crystal of this complex was monoclinic, with a C2 space group and unit cell parameters a = 18.726 Å, b = 24.475 Å, c = 15.398 Å.

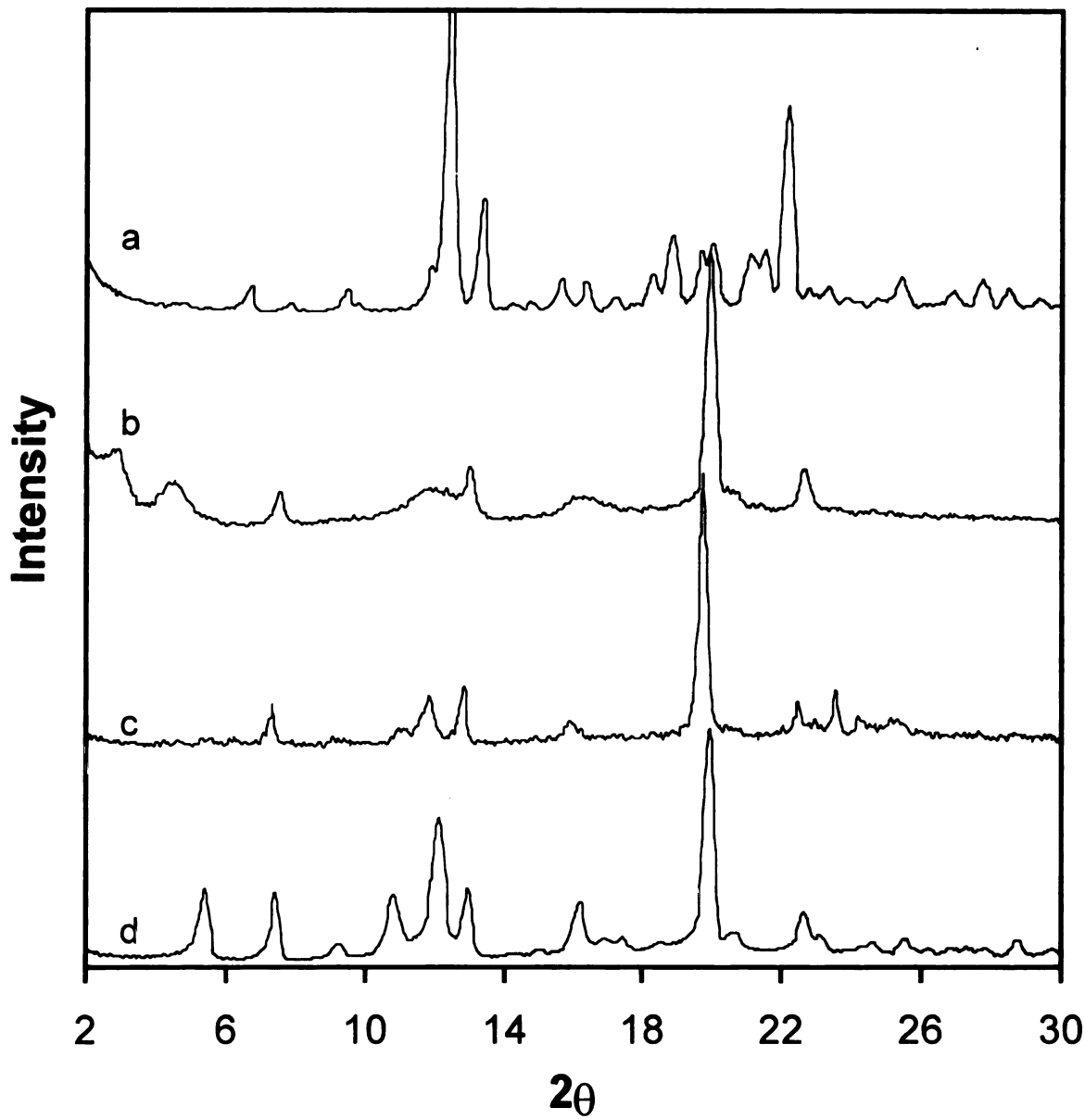

Figure 2.5. Powder X-ray diffraction patterns for α-CD complexes. a) 1-propanol-α-CD, b) $[C_3\pi C_3EO_6]_n$-α-CD, c) $C_{14}EO_8C_{14}$-α-CD, and d) octanol-α-CD. Data were collected at a rate of 2θ = 2°/min over the range 2θ = 0-40°.

Solid-state NMR data also confirmed that polymer chains were threaded through the cyclodextrin cavity. Solid-state NMR probes the structure of the complex at the molecular level and is more sensitive to didordered molecular architectures than powder X-ray diffraction. **Figure 2.6** shows the ^{13}C CP/MAS NMR spectra of the α-CD complexes of $[C_3\pi C_3EO_8]_n$ and $C_{12}EO_{14}C_{12}$, a model compound for the $(AB)_n$ system. Spectra of α-CD, $[C_3\pi C_3EO_8]_n$, and $C_{12}EO_{14}C_{12}$ are shown for comparison. In the uncomplexed state, α-CD exists in an unusual high-energy linkage conformation because one of the glucose residues is rotated toward the axis of the CD torus. This rotation causes the CD molecule to exist in a partially "collapsed" or distorted conformation.[22-24] In this high-energy conformation α-CD is non-symmetrical and thus, the ^{13}C CP/MAS NMR spectrum of α-CD (spectrum a in **Figure 2.6**) shows multiple resonances for each type of carbon in α-CD. Upon complexation with guest molecules, the α-CD macrocycle expands to adopt a nearly symmetrical hexagonal structure, thereby relieving the distorted conformation, which allows each glucose unit of α-CD to exist in a similar environment. ^{13}C CP/MAS NMR spectrum were taken of the individual $(AB)_n$ block copolymer (spectrum e) and the ABA triblock oligomer (spectrum c) to probe for chemical shift changes associated with complexation with α-CD. In the spectrum of $[C_3\pi C_3EO_8]_n$, resonances at ~70 ppm correspond to the carbon atoms of the ethylene oxide block of the polymer, while resonances at ~30 ppm are the methylene carbons of the alkylene block. The spectrum of the triblock oligomer $C_{12}EO_{14}C_{12}$ show similar resonances plus a peak at ~10 ppm from the methyl group of the alkyl blocks. The spectra of the $[C_3\pi C_3EO_8]_n$-α-CD (spectrum d) and $C_{12}EO_{14}C_{12}$-α-CD (spectrum b) ICs show only a broad resonance for each type of carbon atom in the glucose structure, a change

that is consistent with threading of the polymer chain through the CD cavity. These results are consistent with the results of X-ray studies of single crystals of α-CD performed by McMullan and Takeo.[9,25]

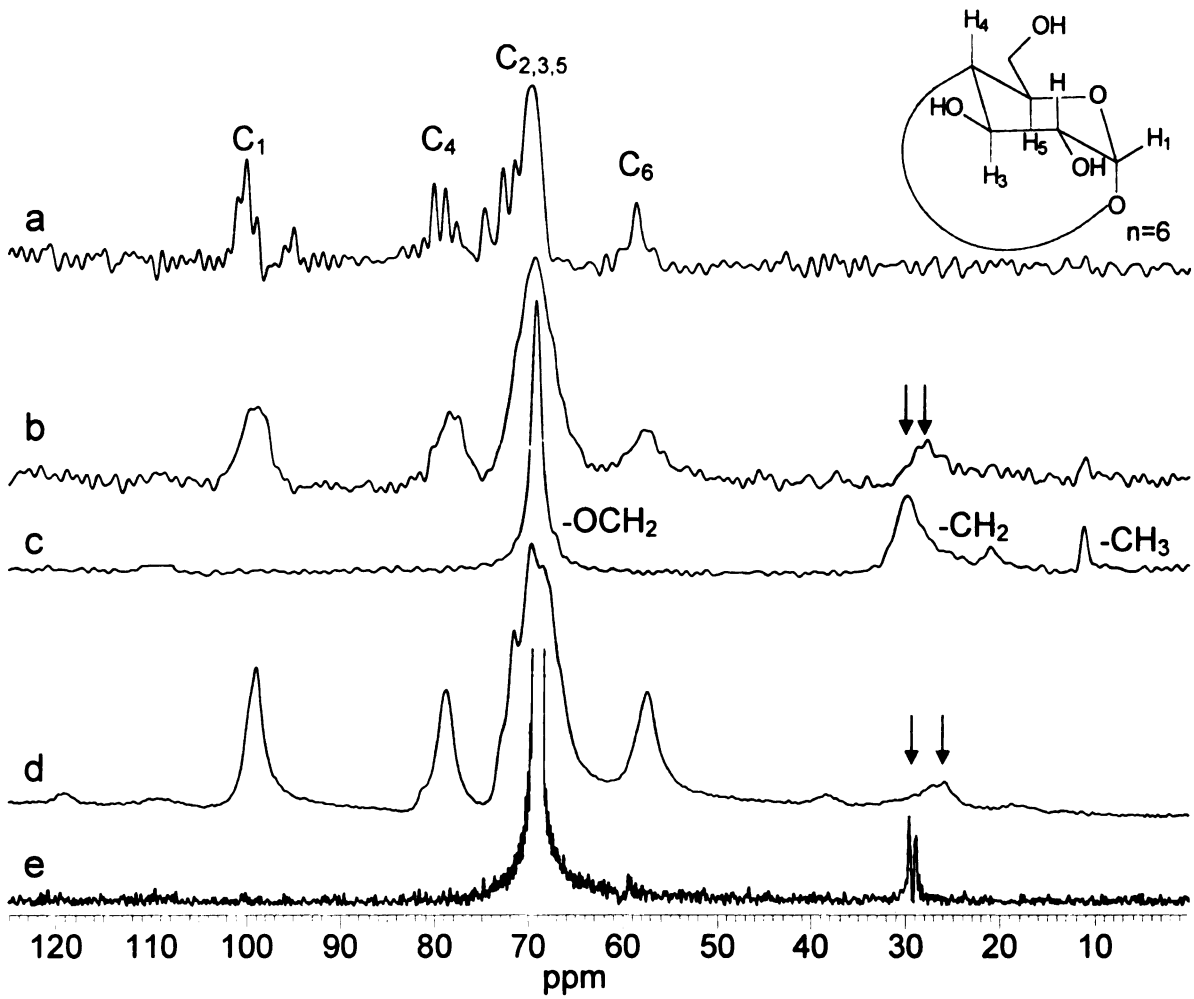

Figure 2.6. ^{13}C CP/MAS NMR spectra of a) α-CD, b) $C_{12}EO_{14}C_{12}$-α-CD, c) $C_{12}EO_{14}C_{12}$, d) $[C_3\pi C_3EO_8]_n$-α-CD, and e)$[C_3\pi C_3EO_8]_n$. Arrows indicate ^{13}C resonances for the alkyl chain of the ABA oligomer that shift when complexed with α-CD. Spectra were taken at a spinning rate of 4.0 KHz.

3) Stoichiometry of complexes

To determine the stoichiometry (number of CD's threaded per polymer repeat unit) of $[C_x\pi C_xEO_y]_n$-α-CD ICs, continuous variation plots were made and the results were compared to stoichiometries determined from ^{1}H NMR spectra of the complexes measured in DMSO-d_6. Harada *et al.* has used this method to determine the stoichiometry of CD complexes of PEO,[4] PCL,[5] and poly(dimethylsiloxane[31]). The continuous variation method (also known as Job's method) is a simple and effective method to determine stoichiometry. Given the chemical reaction:

$$aA + bB \rightleftharpoons cC \qquad \textbf{Equation 2.1}$$

the reaction can be rewritten as:

$$A + kB \rightleftharpoons mC \qquad \textbf{Equation 2.2}$$

where $k = b/a$ and $m = c/a$. If a series of solutions is prepared, each containing the same total number of moles of reactants A (α-CD) and B ($[C_x\pi C_xEO_y]_n$), but with a different mole ratio, R, of B to A, the maximum yield of product C ($[C_x\pi C_xEO_y]_n$-α-CD) is obtained when R = k (the stoichiometric ratio of B to A). A plot of the product yield versus R has a maximum value at the initially unknown value of k.

The method of continuous variation can be justified mathematically through the following procedure. If "x" represent the moles of A in a particular solution, and the total moles of A and B are fixed at 1.0 throughout a series of solutions, then for each solution x = moles of A, and $1-x$ = moles of B. The maximum yield of product is obtained when R = moles B/moles A = $(1-x)/x$, which is equal to k. From **Equation 2.2**, if x is less than the stoichiometric amount of A, then A is the limiting reagent and the moles of the product = mx. A plot of the moles of product versus x over a series of solutions should be

linear, with slope m. If x exceeds the stoichiometric amount of A, then B is the limiting reagent and moles of the product = $m(1-x)/k$. A plot of moles product versus x over a series of solutions should be linear, with slope = $-m/k$. The first plot proceeds up to the right as x increases, while the second plot proceeds down to the right as x increases. At the intersection of these two lines: $mx = m(1-x)/k$, which when solved for x gives: $x = 1/(1+k)$. Substitution for x in the expression of $R = (1-x)/x = \{ 1 - [1/(1+k)]\} / [1/(1+k)] = k$, which demonstrates that the maximum product is obtained when $R = k$.

Figure 2.7 shows continuous variation plots for the same series of $[C_x\pi C_xEO_y]_n$ polymers found in **Figure 2.1**, with the yield of complex plotted as a function of the mole fraction of α-CD. The sum of the reactants was fixed at 1.8×10^{-4} mole (based on the molecular weight of the polymer repeat unit). All of the plots show maximum yields when the molar ratio of α-CD is ~0.70 suggesting that the stoichiometries of the complexes are ~2.3:1 (α-CD : polymer repeat unit).

The stoichiometries obtained from the continuous variation plots agree with those calculated from ^{1}H NMR spectra of the complexes in DMSO-d_6. All $(AB)_n$-α-CD complexes are soluble in DMSO and de-thread in solution. Thus, as shown in the 300 MHz ^{1}H NMR spectra of α-CD, $[C_4\pi C_4EO_8]_n$, and the de-threaded $[C_4\pi C_4EO_8]_n$-α-CD inclusion complex (**Figure 2.8**), the spectra only show resonances for α-CD and the polymer. The stoichiometry of the complex was calculated by comparing the integration values for H-1 of α-CD (see structure in **Figure 2.8**) and the $-CH_2$ (signal 4, α to the C=C bond) of the polymer repeat unit. H-1 of α-CD integrates for six protons while the methylene signal integrates for four protons in the uncomplexed state. In the ^{1}H NMR of

the complex, the same methylene signal integrates for only 1.7 protons, which corresponds to (4.0/1.17) = 2.3 α-CD 's threaded per polymer AB repeat unit.

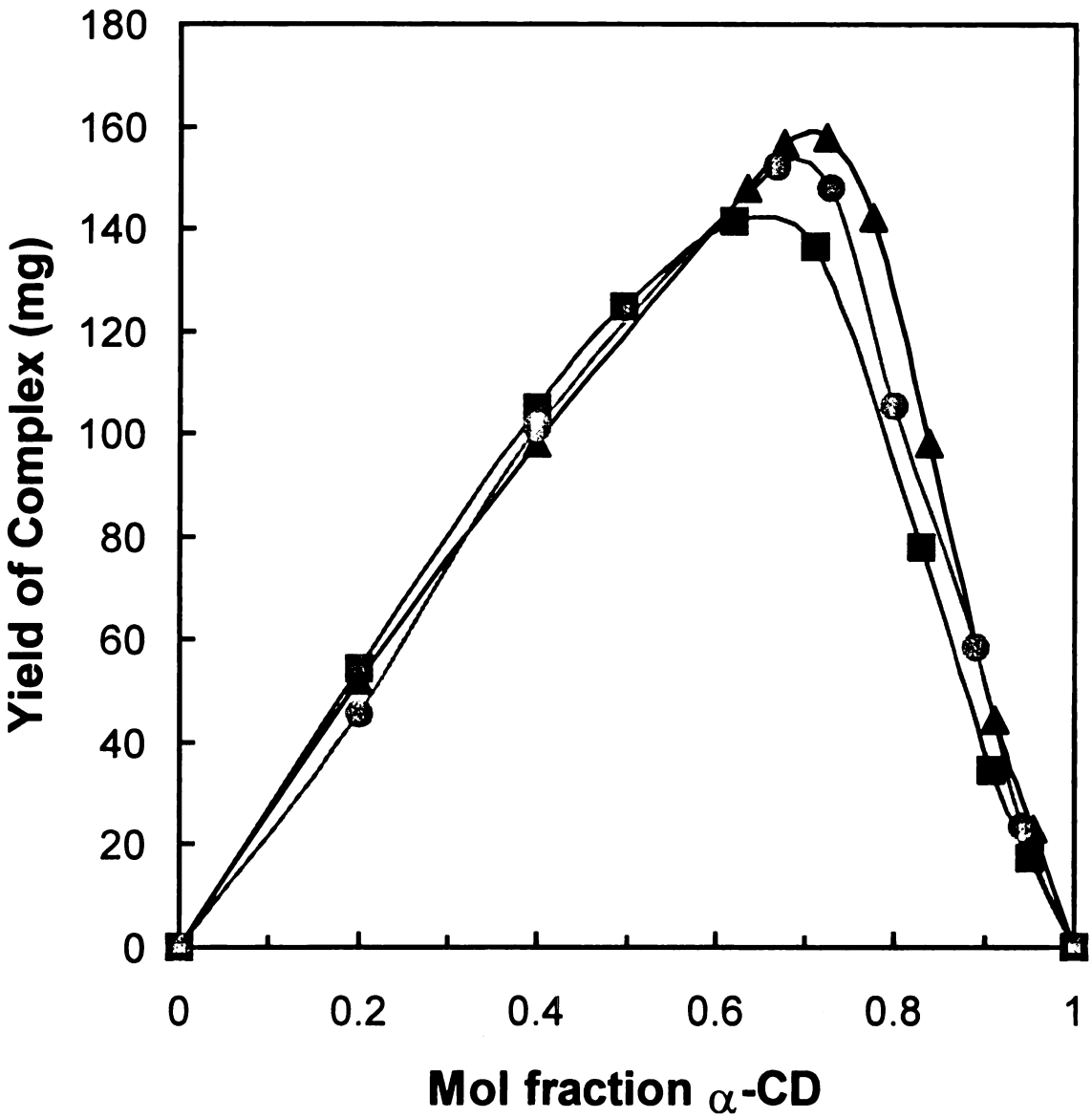

Figure 2.7. Continuous variation plot showing the yield of α-CD/$(AB)_n$ block copolymer complexes obtained for various ratios of reactants. The sum of the reactants was fixed at 1.8×10^{-4} mole (based on the molecular weight of the polymer repeat unit). (■$[C_3\pi C_3EO_8]_n$, ▲ $[C_4\pi C_4EO_8]_n$, ● $[C_3\pi C_3EO_6]_n$).

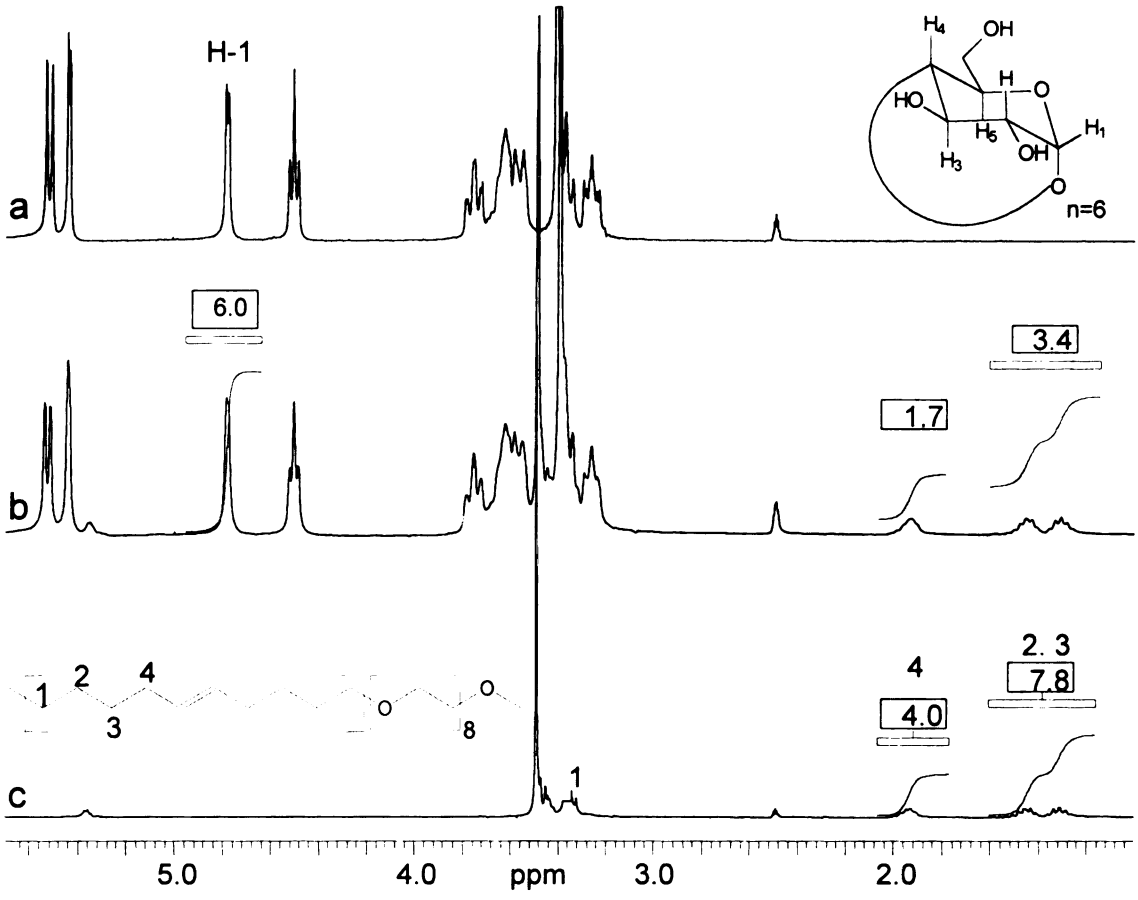

Figure 2.8. The 300 MHz ^{1}H NMR spectrum of a) α-CD, b) the $[C_4\pi C_4EO_8]_n$-α-CD IC, and c) $[C_4\pi C_4EO_8]_n$ in DMSO-d_6. The IC stoichiometry was calculated by comparing the integration ratios of H-1 of α-CD (6 H) to the -CH_2 units (signals 2-4) in the polymer repeat unit.

2.2.3 Complex formation between $C_xEO_yC_x$ model compounds and α-CD

Complexes synthesized from a series of ABA triblock oligomers (**Table 2.2**) were used as model compounds for understanding the behavior of polymer ICs. In particular, $C_xEO_yC_x$-α-CD ICs were synthesized to explore how differences in the hydrophobicity of the model compounds (increased alkyl length or decreased ethylene oxide chain length) affect yield and stoichiometry of the complexes.

Table 2.2. Characteristics of ABA triblock oligomers used to form ICs with α-CD.

ABA triblock	MW (g/mol)	Concentrations of $C_xEO_yC_x$ (mg/mL)
$C_{12}EO_3C_{12}$	486.8	3.3, 6.6, 10, 15, 20, and 33
$C_{12}EO_6C_{12}$	618.9	3.3, 6.6, 10, 15, 20, and 33
$C_{12}EO_8C_{12}$	707.1	3.3, 6.6, 10, 15, 20, 33, and 72.7
$C_{12}EO_{14}C_{12}$	971.4	3.33, 6.6, 10, 15, 20, and 33
$C_{14}EO_3C_{14}$	542.9	8.1, 16.3, and 24.4
$C_{14}EO_6C_{14}$	675.1	10.1, 20.3, 30.4, and 40.5
$C_{14}EO_8C_{14}$	763.2	3.3, 6.6, 10, 15, 20, and 33
$C_{16}EO_3C_{16}$	599.0	9, 18, 27, and 36
$C_{16}EO_6C_{16}$	731.2	11, 22, 33, and 44

When an aqueous solution of α-CD (100 mg/mL) was added to the ABA model compounds above their melting temperature, a white precipitate formed immediately. The solutions were stirred overnight, filtered, washed with water, and dried under vacuum. In contrast to the results seen with the polymers, no gel formed at any concentration of the ABA model compound. Complexes also were synthesized by the dissolution of the model compound in methanol before the addition of the α-CD solution. The yields were lower for this synthetic method, and again no gels formed. As in the polymer case, the yields of the ABA-α-CD ICs were studied as a function of the concentration of ABA model compound. Data for four complexes are shown in **Figure 2.9**. For each series of complexes, the yield saturated at slightly higher concentrations than was seen for the polymers, and at similar concentrations, the isolated yields and saturation levels were higher for the ABA model compounds than for the polymers. The slopes of the plots were similar to that seen for the synthesis of the polymer ICs.

2.2.4 Properties of ABA-α-CD complexes

The $C_xEO_yC_x$-α-CD ICs were analyzed by ^1H and ^{13}C solid-state NMR, powder X-ray diffraction, DSC, and the stoichiometry of the complexes were determined by the continuous variation method. **Figure 2.10** shows a representative continuous variation plot used to determine the number of CDs threaded per $C_{12}EO_8C_{12}$ triblock oligomer. As seen in the figure, the maxima of the plots (0.7 mol fraction α-CD) corresponds to a stoichiometry of 2.3 α-CD's per triblock molecule, similar to that observed for the $(AB)_n$-α-CD ICs. ^1H NMR data confirmed the stoichiometries of the $C_{12}EO_8C_{12}$ and

$C_{12}EO_{14}C_{12}$ complexes; the other ABA model compound-CD complexes were insoluble in deuterated DMSO and all other deuterated solvents tested.

DSC scans were taken of each ABA-α-CD IC and compared to its individual components. A representative example, the $C_{12}EO_8C_{12}$-α-CD IC, (**Figure 2.11**) shows a melting transition at 33°C for the triblock oligomer, which is lost upon complexation with α-CD. The scan of the complex is featureless like that of α-CD, confirming that there is no free ABA compound in the samples. To further prove that α-CD was threaded onto the model compounds, the ABA-α-CD ICs were analyzed by powder X-ray diffraction and ^{13}C solid-state NMR. **Figure 2.5** (trace c) shows a representative example, the $C_{14}EO_8C_{14}$-α-CD IC, which has a diffraction pattern consistent with the formation of columnar (channel) crystal structure. ^{13}C solid-state CP/MAS NMR (**Figure 2.6**) was taken of the triblock oligomer, $C_{14}EO_{12}C_{14}$ (spectrum C), and its inclusion complex with α-CD (spectrum B). Like the $(AB)_n$-α-CD ICs, α-CD becomes symmetrical in the inclusion complex formation with the ABA model compounds, a change that is consistent with threading of triblock oligomer through the CD cavity.

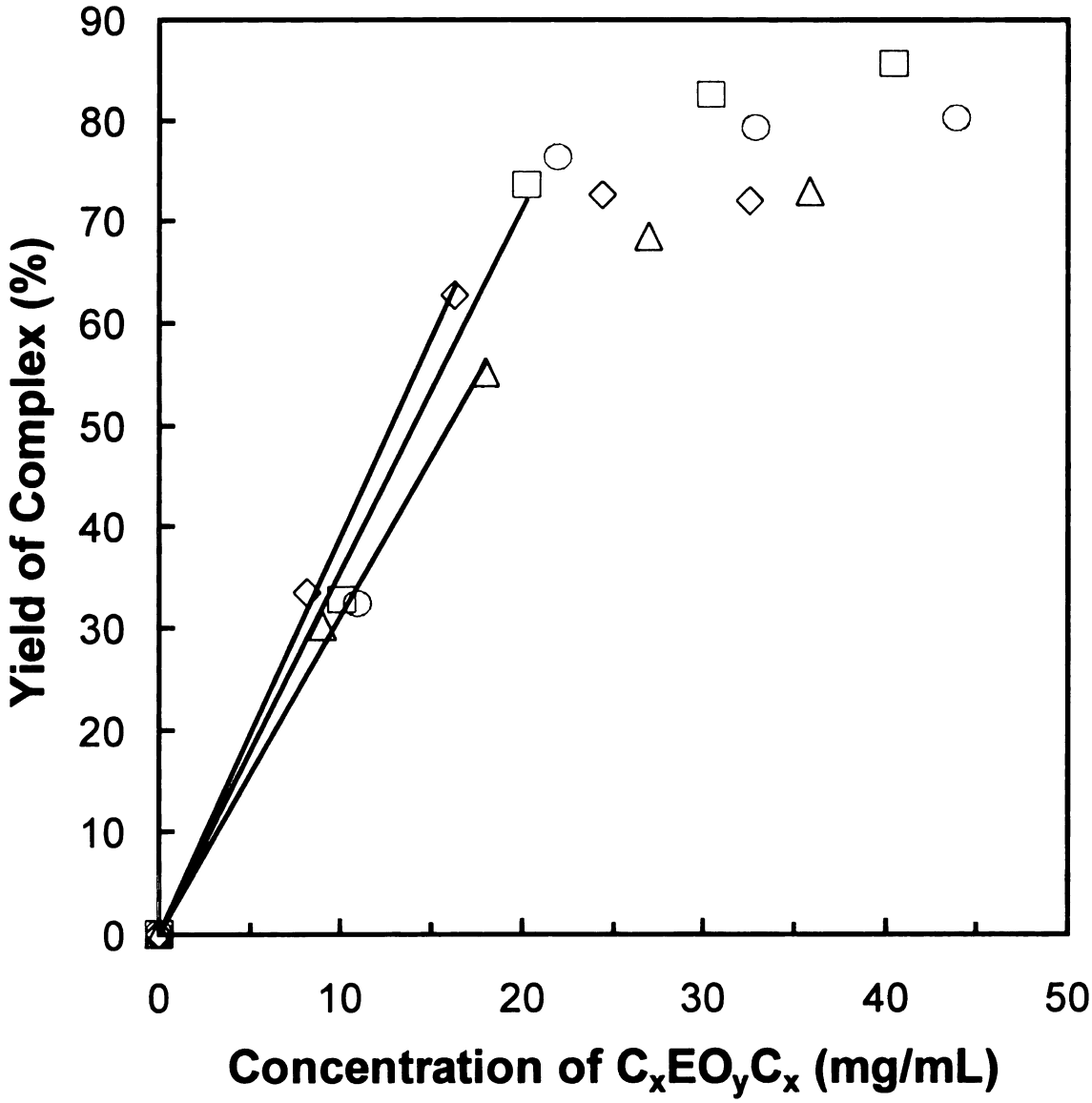

Figure 2.9. Yield of $C_xEO_yC_x$-α-CD complex as a function of the ABA triblock concentration. Complexes were prepared by adding an aqueous solution of α-CD (150 mg/1.0 mL H_2O) to the molten ABA oligomer (5 – 60 mg).
(□ $C_{14}EO_6C_{14}$, Δ $C_{16}EO_3C_{16}$, ○ $C_{16}EO_6C_{16}$, ◇ $C_{14}EO_3C_{14}$).

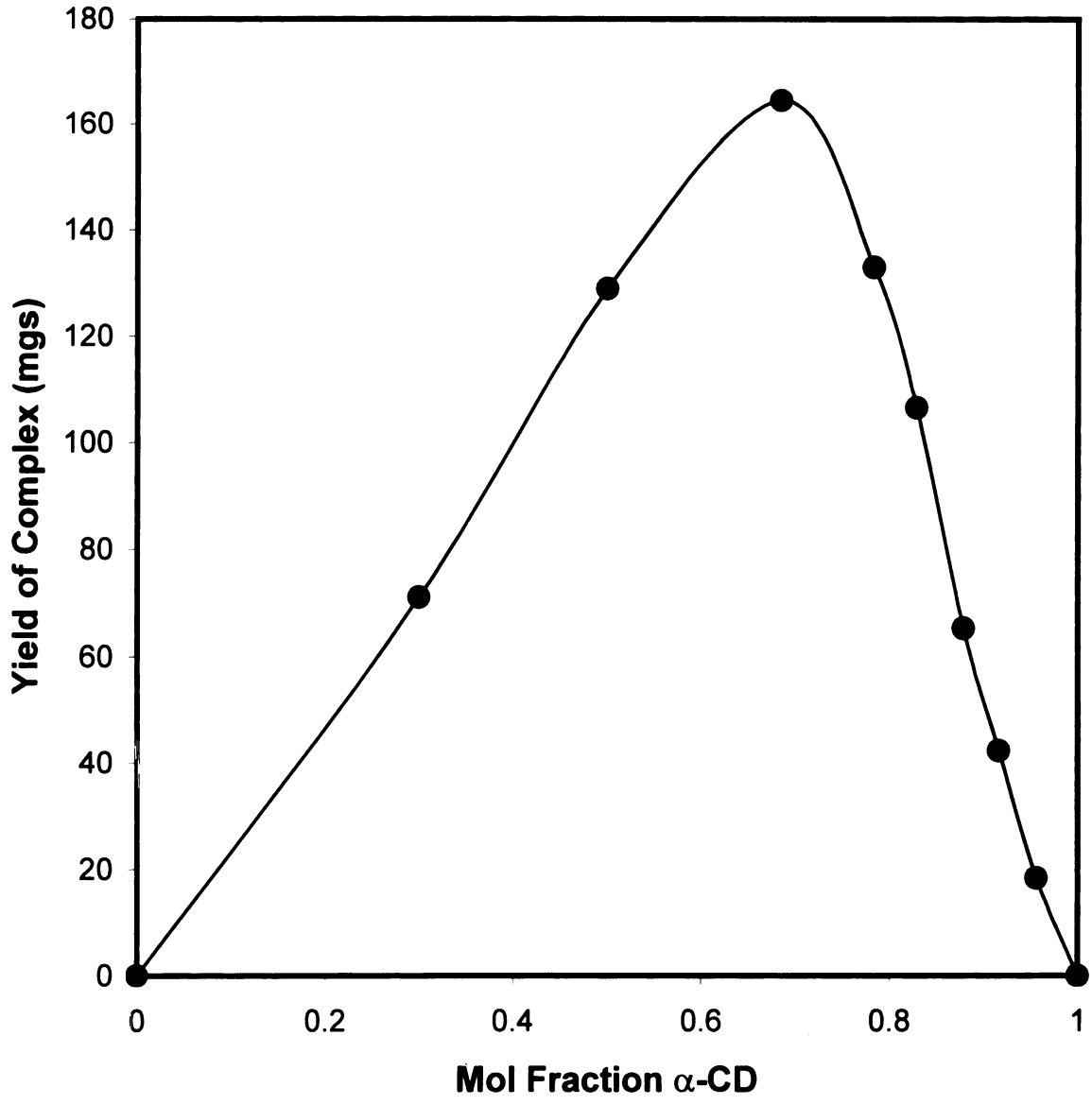

Figure 2.10. Continuous variation plot showing the yield of the $C_{12}EO_8C_{12}$-α-CD IC (●) obtained for various ratios of the reactants. The sum of the reactants was fixed at 1.5 × 10^{-4} mole.

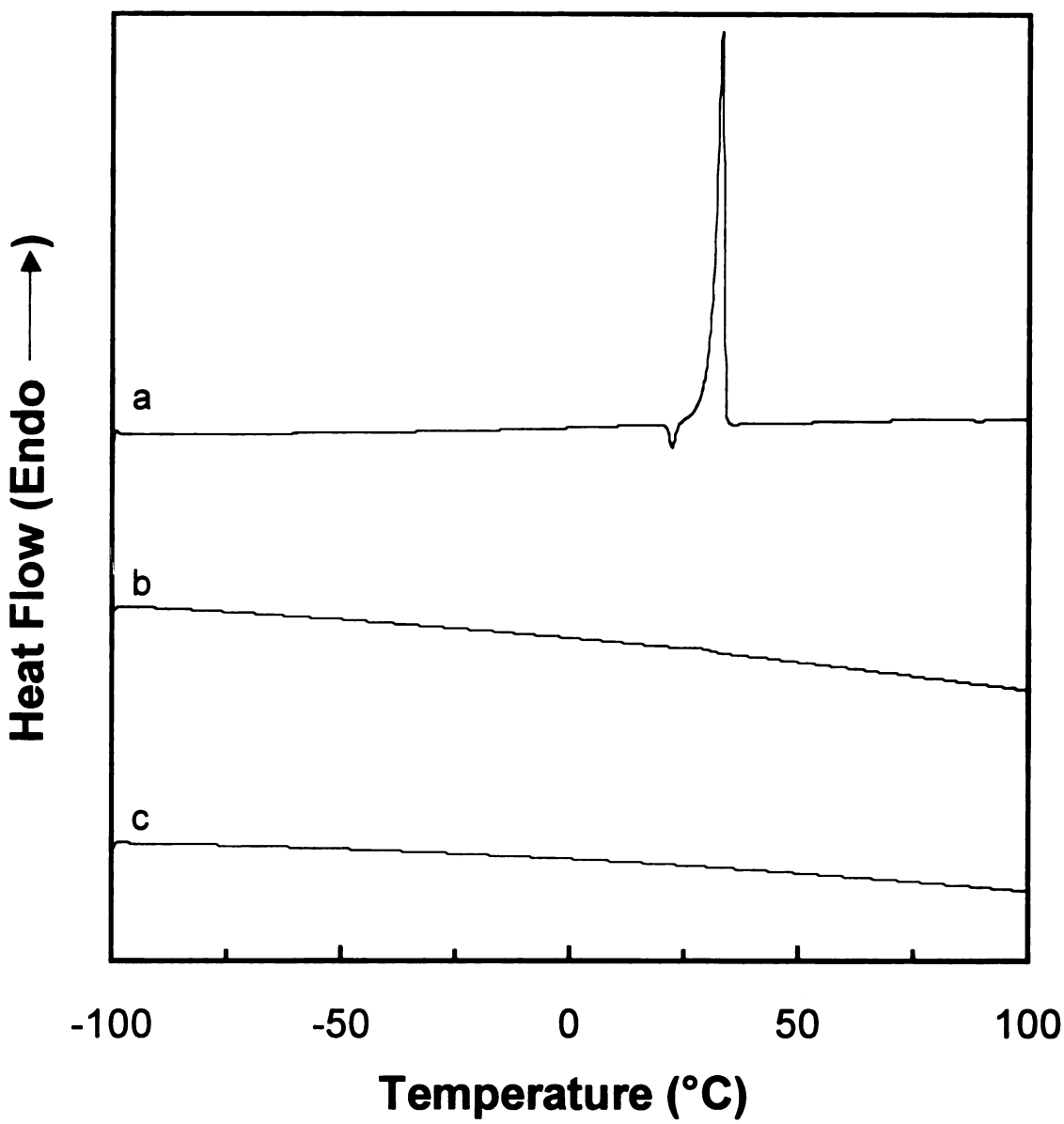

Figure 2.11. Normalized DSC thermograms of a) $C_{12}EO_8C_{12}$, b) $C_{12}EO_8C_{12}$-α-CD IC, and c) α-CD. The scans shown are the second heating scans taken after heating the samples to 100°C to erase the thermal history, and flash quenching to -100°C. All scans were run at 10°C/min under helium.

2.3 Discussion

Since the discovery by Harada that α-CD threads onto a polyethylene glycol chain,[1] numerous inclusion complexes have been synthesized from a wide variety of polymers. The design of nanometer scale supramolecular structures organized by noncovalent interactions in the hydrophobic cavity of CD has gained much interest by many researchers. Besides studying the noncovalent binding forces (found in biological systems), the selectivity and molecular recognition of CD towards guest molecules has been of major interest. Molecular recognition is based on the selectivity-structure correlation between the host cavity of CD and the guest-solvent mixture. Previous researchers have shown α-CD can recognize guest molecules based on the cross-sectional areas of the polymer. Harada has shown that α-CD will form ICs with PEG, but will not form complexes with PPG because of size constraints of the polymer backbone.[26] A goal of this research was to see if α-CD could distinguish (recognize) between two types of polymers based on their difference of properties, not in size.

To date there have been few reports of ICs formed from block copolymers. Such complexes could have interesting structures and properties since the CDs could preferentially thread onto one of the blocks. Tonelli *et al.* prepared α and γ-CD complexes with a (PCL-PEO-PCL) ABA triblock copolymer,[16] to study the behavior of isolated and segregated polymer chains. Since only a single chain can be incorporated inside the α-CD cavity and two parallel, side-by-side chains can reside in the γ-CD channel, one can compare properties of single and pairs of parallel, side-by-side chains with those of the bulk polymer. Yui *et al.* synthesized stimuli-responsive polyrotaxanes from β-CD and a PEO-PPO-PEO triblock copolymer that can function as a molecular

piston,[27,28] and Topchieva *et al.* studied complex formation with a series of low molecular weight nonionic surfactants: PEO-PPO, PEO-PPO-PEO, and PPO-PEO-PPO[29].

In this research, we reported the first synthesis of α-cyclodextrin ICs with $(AB)_n$ microblock copolymers. The structures of these high molecular weight polymers are related to nonionic surfactants, and differ in that the blocks have relatively short lengths and the AB pattern is repeated many times. We also reported results for a series of ABA triblock model compounds[30] that have structures similar to the $(AB)_n$ block copolymers. The ICs formed from these small molecule analogs helped in interpreting the results obtained for the α-CD complexes of $(AB)_n$ block copolymers.

2.3.1 Solid state ^{13}C NMR of inclusion complexes

The experimental data show that α-CD threads onto the $(AB)_n$ and ABA model compounds to form columnar inclusion complexes, and the NMR results support a facile threading and de-threading process in solution. There is however, inconclusive evidence for selectivity in the threading process. One would expect that α-CD would prefer to reside over the hydrophobic segments of the polymer chain. One sign of selective threading would be a shift in the ^{13}C resonances for the alkyl chains, without a corresponding change in the signal from the carbon atoms of the ethylene oxide chains. The solid state NMR spectrum of $[C_3\pi C_3EO_8]_n$ (**Figure 2.6**, spectrum e) shows a sharp resonance at about 29 ppm from the methylene units of the alkylene blocks and a peak at 69 ppm from the ethylene oxide units of the polymer chain. In the spectrum of the $[C_3\pi C_3EO_8]_n$-α-CD complex (spectrum d), the methylene resonance broadens and shifts to 26 ppm. The results for the ABA model system are similar; the ^{13}C resonances for the

alkyl chain shift from 30 ppm in the ABA oligomer to 28 ppm in the α-CD complex. However, the ethylene oxide signals in the $(AB)_n$ block copolymers and ABA model compounds overlap with the signals observed for carbons C-2, C-3, and C-5 of α-CD, which makes any changes in the chemical shift for these resonances unobservable.

2.3.2 Stoichiometry of inclusion complexes

The stoichiometry of the polymer-α-CD complexes studied was 2.3 α-CD units/polymer repeat unit. The same stoichiometry was obtained for complexes prepared from the ABA model compounds. Comparisons of the length of the polymer repeat unit with the depth of the α-CD cavity (8 Å) suggest a maximum threading of 6-7 α-CD units/repeat unit. The low observed stoichiometry suggests that the CD units are not threaded uniformly onto the polymer, due to kinetic control of the stoichiometry of the complex. Considering the solid state NMR results and the stoichiometry of the complexes, we conclude that our data are consistent with preferential threading onto the alkylene segments.

Non-uniform threading can stem from the precipitation of the complex from solution, and the data of **Figure 2.1** implicate solubility as a major factor in determining the yield and stoichiometry of the complexes. The yield plots for the polymers show slightly different slopes that depend on the mole fraction of the hydrophobic alkylene chain in the polymer. In **Figure 2.1**, the least hydrophobic polymer ($[C_3\pi C_3EO_8]_n$, 8 of 33 chain atoms in the alkylene segment) has the smallest slope and the lowest yield at saturation. The other two polymers, $[C_3\pi C_3EO_6]_n$ and $[C_4\pi C_4EO_8]_n$, are essentially identical in terms of the fraction of chain atoms in the hydrophobic segment, and have

slopes and limiting yields that are nearly identical. For the IC stoichiometry to be nearly independent of the polymeric or ABA model compound structure, the solubility limit for the ICs must be exceeded when 2-3 α-CD units thread onto the chain. Since the amphiphilic nature of the polymers renders the $(AB)_n$ polymers sparingly soluble in the reaction solvent, it should not be surprising that threading a few CD units onto a chain is sufficient to make the IC insoluble.

An alternative explanation for the shift of the slope in **Figure 2.1**, is a molecular weight dependence on the threading rate. Of the three polymers used in the study, $[C_3\pi C_3EO_8]_n$ had the highest molecular weight (M_n= 44 kg/mol) whereas those of $[C_4\pi C_4EO_8]_n$ and $[C_3\pi C_3EO_6]_n$ were lower (M_n= 19 and 25 kg/mol, respectively). Thus consistent with the results, $[C_3\pi C_3EO_8]_n$ should be the slowest polymer to completely thread and might be expected to give the lowest yield. A molecular weight effect is not observed in the ABA triblock model compound series (**Figure 2.9**) nor when ICs were made at the same concentration with various $(AB)_n$ polymers that have different M_n's (data not shown). A molecular weight effect cannot be ruled out though because samples covering a broad range of molecular weights were not available for this study.

2.4 Conclusions

A variety of spectroscopic and analytical techniques confirm that α-CD threads onto $(AB)_n$ microblock copolymers and ABA triblock model compounds to give columnar inclusion complexes. Relatively small changes are seen in the yield and stoichiometry of the complexes as the lengths of A and B units are changed. The stoichiometry of the complexes is dominated by the decrease in the solubility of the

polymers upon complexation. Solid state NMR data on complexes formed from ABA triblock model compounds suggest preferential threading over hydrophobic segments, although the 2.3:1 stoichiometry observed for the complexes does not lead to a simple regular structure for the complexes.

2.5 References

(1) Harada, A.; Kamachi, M. *Macromolecules* **1990**, *23*, 2821-2823.

(2) Ceccato, M.; LoNostro, P.; Baglioni, P. *Langmuir* **1997**, *13*, 2436-2439.

(3) Qiao, J.; Chen, Y. Y.; Baker, G. L. *Chemistry of Materials* **1999**, *11*, 2542-2547.

(4) Harada, A.; Li, J.; Kamachi, M. *Macromolecules* **1993**, *26*, 5698-5703.

(5) Kawaguchi, Y.; Nishiyama, T.; Okada, M.; Kamachi, M.; Harada, A. *Macromolecules* **2000**, *33*, 4472-4477.

(6) Rusa, C. C.; Luca, C.; Tonelli, A. E. *Macromolecules* **2001**, *34*, 1318-1322.

(7) Rusa, C. C.; Tonelli, A. E. *Macromolecules* **2000**, *33*, 1813-1818.

(8) Harada, A.; Li, J.; Kamachi, M.; Kitagawa, Y.; Katsube, Y. *Abstracts Papers of the American Chemical Society* **1997**, *213*, 28-POLY.

(9) McMullan R.K.; Saenger. W.; Fayos J.; Mootz D. *Carbohydrate Research* **1973**, *31*, 37.

(10) Saenger, W. *Angewandte Chemie-International Edition in English* **1980**, *19*, 344-362.

(11) Saenger, W. R.; Jacob, J.; Gessler, K.; Steiner, T.; Hoffmann, D.; Sanbe, H.; Koizumi, K.; Smith, S. M.; Takaha, T. *Chemical Reviews* **1998**, *98*, 1787-1802.

(12) Harata, K. *Chemical Reviews* **1998**, *98*, 1803-1827.

(13) Saenger, W.; McMullan, R. K.; Fayos, J.; Mootz, D. *Acta Crystallography, Sect. B* **1974**, *B30*, 2019-28.

(14) Panova, I. G.; Gerasimov, V. I.; Topchieva, I. N. *Vysokomolekulyarnye Soedineniya Seriya A & Seriya B* **1998**, *40*, 1681-1686.

(15) Harada, A. *Coordination Chemistry Reviews* **1996**, *148*, 115-133.

(16) Lu, J.; Shin, I. D.; Nojima, S.; Tonelli, A. E. *Polymer* **2000**, *41*, 5871-5883.

(17) Huh, K. M.; Ooya, T.; Sasaki, S.; Yui, N. *Macromolecules* **2001**, *34*, 2402-2404.

(18) Harada, A.; Suzuki, S.; Okada, M.; Kamachi, M. *Macromolecules* **1996**, *29*, 5611-5614.

(19) Li, J.; Yan, D. *Macromolecules* **2001**, *34*, 1542-1544.

(20) Lu, J.; Mirau, P. A.; Tonelli, A. E. *Macromolecules* **2001**, *34*, 3276-3284.

(21) Udachin, K. A.; Wilson, L. D.; Ripmeester, J. A. *Journal of the American Chemical Society* **2000**, *122*, 12375-12376.

(22) Manor, P. C.; Saenger W. *Journal of the American Chemical Society* **1974**, *1974*, 3630-3639.

(23) Gidley, M. J.; Bociek, S. M. *Journal of the American Chemical Society* **1988**, *110*, 3820-3829.

(24) Schneider, H. J.; Hacket, F.; Rudiger, V.; Ikeda, H. *Chemical Reviews* **1998**, *98*, 1755-1785.

(25) Takeo, K.; Kuge, T *Agricultural and Biological Chemistry* **1970**, *34*, 1787.

(26) Harada, A.; Okada, M.; Kawaguchi, Y.; Kamachi, M. *Polymers For Advanced Technologies* **1999**, *10*, 3-12.

(27) Fujita, H.; Ooya, T.; Yui, N. *Macromolecules* **1999**, *32*, 2534-2541.

(28) Fujita, H.; Ooya, T.; Yui, N. *Macromolecular Chemistry and Physics* **1999**, *200*, 706-713.

(29) Topchieva, I. N.; Karezin, K. I. *Colloid Journal* **1999**, *61*, 514-519.

(30) Chen, Y. Y.; Baker, G. L. *Journal of Organic Chemistry* **1999**, *64*, 6870-6873.

(31) Okumura, H.; Okada, M.; Kawaguchi, Y.; Harada A. *Macromolecules* **2000**, *33*, 4297-4298.

CHAPTER 3

Experimental

3.1 General details

Unless otherwise specified, ACS reagent grade starting materials were used as received from commercial suppliers. THF was dried by refluxing over CaH_2 overnight, and was then distilled from Na/benzophenone. House nitrogen was used in air and moisture sensitive reactions.

Proton and carbon nuclear magnetic resonance (^1H and ^{13}C) analyses were carried out at room temperature in deuterated solvents ($CDCl_3$, DMSO-d_6, and D_2O) on a Varian Gemini-300 spectrometer. The chemical shifts were calibrated using the signals from residual non-deuterated solvent and are reported relative to tetramethylsilane. Solid-state ^{13}C CP/MAS NMR spectra were measured at 100.4 MHz on a Varian VXR-400 spectrometer with sample spinning rates of 4 0 kHz at room temperature.

Molecular weights of polymer samples were determined by gel permeation chromatography (GPC) using a PLgel 20μ Mixed A column at 30 °C with THF as eluting solvent at a flow rate of 1mL/min. A Waters R410 Differential Refractometer was used as the detector. The concentration of the polymer samples was 1mg/mL, and the results were calibrated with monodisperse polystyrene standards.

Differential scanning calorimetry (DSC) analyses of compounds were run on a Perkin Elmer DSC 7 instrument calibrated with indium and hexyl bromide standards. The samples were sealed in aluminum pans and were heated at 10°C/min under a helium atmosphere. Liquid nitrogen was used as a coolant. Samples were melted and held at 150°C for five minutes to erase their thermal history. They then were quenched to –100

°C at a rate of 200°C/min, and then held at −100°C for five minutes before the sample run was started. Samples were heated to 150°C, cooled to −100°C, and heated to150°C, all at a rate of 10°C/min. The DSC melting point was taken as the onset of the peak of the melting endotherm. Heats of fusion were calculated from the endothermic peak using the accompanied functions of the DSC 7 software. Thermogravimetric analyses (TGA) of the compounds were obtained from a Perkin Elmer TGA 7 instrument at a heating rate of 10°C/min, usually over the temperature range of 30 to 600°C.

X-ray diffraction patterns were collected from powdered samples on a Rigaku rotaflex 200B diffractometer equipped with a rotating anode, Cu Kα x-ray radiation (λ=1.541838 Å) and a curved crystal graphite monochrometer. Diffraction patterns were collected at a rate of 2θ = 2°/min over the range 2θ = 0-40°. Powdered samples were prepared by grinding the samples and then spreading the solid onto the window of a glass sample holder with a spatula.

3.2 Material synthesis

The $(AB)_n$ polymers were prepared by the metathesis polymerization (ADMET) of oligoethylene oxide α,ω-dialkenyl ethers using Schrock's molybdenum alkylidene catalyst as described earlier.[1-3] The number average molecular weights (M_n) of the polymers were $[C_4\pi C_4EO_8]_n$ = 19×10^3, $[C_3\pi C_3EO_8]_n$ = 44×10^3, and $[C_3\pi C_3EO_6]_n$ = 25×10^3 g/mol. The polydispersity of each polymer is ~2. The polymers are soluble in methanol and THF, but are insoluble in hexanes and water. ABA triblock oligomers were prepared by treating the appropriate exact length oligoethylene glycol with NaH and 2 equivalents of the desired alkyl bromide.

1 Complex Formation between $[C_x\pi C_xEO_y]_n$ Polymers and α-CD.

Inclusion complexes of α-CD and $[C_x\pi C_xEO_y]_n$ polymers were prepared at room temperature by adding a 2 mL solution of α-CD in water to a solution of the $(AB)_n$ block copolymer in 0.5 mL methanol. For low polymer concentrations (< 8 mg/mL), the solution became turbid and the complex precipitated as white crystals, which were collected by filtration and washed with water to remove any uncomplexed α-CD. All complexes were dried overnight in a vacuum oven to remove any water from the complex. Higher polymer concentrations led to formation of a white gel, which was isolated as a crystalline inclusion complex by freeze-drying and washing the resulting solid with water.

2 Complex Formation between $C_xEO_yC_x$ model compounds and α-CD.

Complexes were synthesized from three series of model compounds, $C_{12}EO_yC_{12}$ where y= 3, 6, 8, and 14, $C_{14}EO_yC_{14}$ where y = 3, 6, and 8, and $C_{16}EO_yC_{16}$ where y = 3 and 6, to explore how the differences in the hydrophobicity of the model compounds (increased alkyl length or decreased ethylene oxide chain length) have on the complex yield and stoichiometry of the complexes. When an aqueous solution of α-CD (100 mg/mL) was added to the ABA model compounds above their melting temperature, a white precipitate formed immediately. The solutions were stirred overnight, filtered, washed with water, and dried under vacuum.

3.3 References

(1) Qiao, J.; Chen, Y. Y.; Baker, G. L. *Chemistry of Materials* **1999**, *11*, 2542-2547.

(2) Chen, Y. Y.; Baker, G. L. *Journal of Organic Chemistry* **1999**, *64*, 6870-6873.

(3) Chen, Y. Y.; Baker, G. L.; Ding, Y. Q.; Rabolt, J. F. *Journal of the American Chemical Society* **1999**, *121*, 6962-6963.